AD-755 376

PROPELLANT IMPROVEMENT PROGRAM. VOLUME II. IRON CONTAMINATION EFFECT IN HDA (HIGH DENSITY ACID)

A. H. Blessing, et al

Bell Aerospace Company

Prepared for:

Air Force Rocket Propulsion Laboratory

January 1973

DISTRIBUTED BY:

NTIS

National Technical Information Service
U. S. DEPARTMENT OF COMMERCE
5285 Port Royal Road, Springfield Va. 22151

AD753376

AFRPL-TR-73-7

PROPELLANT IMPROVEMENT PROGRAM

Volume II - Iron Contamination Effect in HDA

A.H. Blessing and H. J. Loftus

Bell Aerospace Company
P.O. Box 1
Buffalo NY 14240

TECHNICAL REPORT AFRPL-TR-73-7

January 1973

Special Technical Report for Period 1 March 1972 - 31 October 1972

Approved for public release; distribution unlimited

AIR FORCE ROCKET PROPULSION LABORATORY
Director of Science and Technology
Air Force Systems Command
United States Air Force
Edwards, California

NOTICES

When U.S. Government drawings, specifications, or other data are used for any purpose other than a definitely related Government procurement operation, the Government thereby incurs no responsibility nor any obligation whatsoever, and the fact that the Government may have formulated, furnished, or in any way supplied the said drawings, specifications, or other data, is not to be regarded by implication or otherwise, or in any manner licensing the holder or any other person or corporation, or conveying any rights or permission to manufacture, use, or sell any patented invention that may in any way be related thereto.

UNCLASSIFIED

Security Classification

DOCUMENT CONTROL DATA - R & D

(Security classification of title, body of abstract and indexing annotation must be entered when the overall report is classified)

1. ORIGINATING ACTIVITY (Corporate author) Bell Aerospace Company P.O. Box 1 Buffalo, New York 14240	2a. REPORT SECURITY CLASSIFICATION Unclassified 2b. GROUP

3. REPORT TITLE

PROPELLANT IMPROVEMENT PROGRAM

Volume II - Iron Contamination Effects in HDA

4. DESCRIPTIVE NOTES (Type of report and inclusive dates)

Special Technical Report

5. AUTHOR(S) (First name, middle initial, last name)

A. H. Blessing, H. J. Loftus

6. REPORT DATE January 1973	7a. TOTAL NO. OF PAGES	7b. NO. OF REFS

8a. CONTRACT OR GRANT NO. F04611-72-C-0026 b. PROJECT NO. 3058 c. d.	9a. ORIGINATOR'S REPORT NUMBER(S) AFRPL-TR-73-7 9b. OTHER REPORT NO(S) (Any other numbers that may be assigned this report) Bell Aerospace Company Report No. 8643-928002

10. DISTRIBUTION STATEMENT

Approved for public release; distribution unlimited.

11. SUPPLEMENTARY NOTES	12. SPONSORING MILITARY ACTIVITY Air Force Rocket Propulsion Laboratory, Edwards Air Force Base California 93523

13. ABSTRACT

The objectives of this task were to establish the forced convection heat transfer characteristics of Standard and Modified High Density Acid (HDA) and the effect of iron impurity level up to 100 parts per million as Fe_2O_3 on HDA heat transfer.

Thirty tests were conducted utilizing resistance heated, circular, 6061T6 aluminum tubes. Results showed that normal nucleate boiling did not occur with either of the HDA compositions. As the tube wall temperature increased above 300°F it was generally observed that heat transfer was adversely affected. This effect was manifested by an increased thermal resistance which resulted in generally higher wall temperature to support a given heat flux.

The experimental forced convection heat transfer coefficients were unaffected by iron impurity level and exhibited increased values with increased bulk temperature.

Modified HDA when compared to Standard HDA produced about 10% lower heat transfer coefficients and somewhat higher heat flux at tube destruction.

DD FORM 1 NOV 65 1473

UNCLASSIFIED

Security Classification

14 KEY WORDS	LINK A		LINK B		LINK C	
	ROLE	WT	ROLE	WT	ROLE	WT
Liquid Propellant Rocket Oxidizers						
High Density Acid						
Heat Transfer						
Rocket Engine						

AFRPL-TR-73-7

PROPELLANT IMPROVEMENT PROGRAM

Volume II - Iron Contamination Effects in HDA

A. H. Blessing and H. J. Loftus

1C

FOREWORD

This report covers the performance of Task II of the Propellant Improvement Program - Iron Contamination Effects in High Density Acid. The task was performed by Bell Aerospace during the period 1 March 1972 to 31 October 1972 for the Air Force Rocket Propulsion Laboratory, Liquid Rocket Division, Edwards Air Force Base, California. The work, performed in satisfaction of Air Force Contract FO4611-72-C-0026 was under the direction of Air Force Project Engineer, Lt. J. J. Bon, LKDP.

The BAC Project Manager/Technical Director was Mr. H. Joseph Loftus. Other principal contributors in accomplishing the work were:

A. H. Blessing	R. Kubis
N. Engel	E. E. Seymour
H. Ph. Heubusch	J. C. Tynan
R. D. Kalp	T. F. Zack

This report was submitted and approved by H. Joseph Loftus. The contractor's secondary report number is 8643-928002.

This technical report has been reviewed and is approved.

J. J. Bon 1st Lt. USAF
Project Engineer

ABSTRACT

The objectives of this task were to establish the forced convection heat transfer characteristics of standard and modified High Density Acid (HDA) and the effect of iron impurity level up to 100 parts per million as Fe_2O_3 on HDA heat transfer.

Thirty tests were conducted utilizing resistance heated, circular, 6061T6 aluminum tubes. Results showed that normal nucleate boiling did not occur with either of the HDA compositions. As the tube wall temperature increased above 300°F it was generally observed that heat transfer was adversely affected. This effect was manifested by an increased thermal resistance which resulted in generally higher wall temperature to support a given heat flux.

The experimental forced convection heat transfer coefficients were unaffected by iron impurity level and exhibited increased values with increased bulk temperature.

Modified HDA when compared to Standard HDA, produced about 10 percent lower heat transfer coefficients and somewhat higher heat flux at tube destruction.

CONTENTS

Section			Page
1.0	INTRODUCTION		1
2.0	SUMMARY, CONCLUSIONS, AND RECOMMENDATIONS		
	2.1	Summary	1
	2.2	Conclusions	1
	2.3	Recommendations	2
3.0	TECHNICAL DISCUSSION		3
	3.1	Test Plan	3
	3.2	Test Specimen	4
	3.3	Test Apparatus	4
	3.4	Test Instrumentation	6
	3.5	Test Procedure	7
	3.6	Data Reduction	7
	3.7	Description of the Heat Transfer Process	9
	3.8	Test Results	10
	3.8.1	Effect Of Iron Impurity Level	11
	3.8.2	Effect Of Inlet Temperature	13
	3.8.3	Effect Of Velocity	14
	3.8.4	Analysis Of Test Results	14
	3.9	Application To Agena Thrust Chamber	15
4.0	REFERENCES		16

ILLUSTRATIONS

Figure		Page
1	Tube Test Specimen Assembly	17
2	Heat Transfer Tube Specimen Prior To Final Flame Spray	18
3	Completed Heat Transfer Tube Specimen	19
4	Shutdown Simulation Test Sequence	20
5	Heat Transfer Test Apparatus Characteristics	21
6	Forced Convection Heat Transfer Test Cell No. X-1 Schematic	22
7	Test Apparatus - Left Side View	23
8	Test Apparatus - Right Side View	24
9	Forced Convection Heat Transfer Process	25
10	Heat Flux Versus Wall Temperature - Test 1199	26
11	Effect Of Shutdown On Heat Transfer With Standard HDA Containing 30 PPM Iron Contaminant	27
12	Effect Of Shutdown On Heat Transfer With Standard HDA Containing 55 PPM Iron Contaminant	28
13	Effect Of Shutdown On Heat Transfer With Standard HDA Containing 72 PPM Iron Contaminant	29
14	Effect Of Shutdown On Heat Transfer With Standard HDA Containing 96 PPM Iron Contaminant	30
15	Effect Of Shutdown On Heat Transfer With Modified HDA (0.55% PF_5) Containing 10 PPM Iron Contaminant	31
16	Effect Of Shutdown On Heat Transfer With Modified HDA (0.55% PF_5) Containing 50 PPM Iron Contaminant	32
17	Effect Of Shutdown On Heat Transfer With Modified HDA (0.55% PF_5) Containing 97 PPM Iron Contaminant	33
18	Effect Of Temperature On Heat Transfer Coefficient	34
19	Effect Of Shutdown On Heat Transfer With Modified HDA (0.55% PF_5) Containing 92 PPM Iron Contaminant	35
20	HDA Composite Coolant Characteristic	36
21	Agena Thrust Chamber Wall Element At Throat Station	37

TABLES

Number		Page
I	HDA Composition (Weight %)	38
II	Test Matrix	39
III	Measured And Derived Data	40
IV	Summary Of HDA Heat Transfer Tests	49

LIST OF ABBREVIATIONS AND SYMBOLS

Symbol or Abbreviation	Description Or Meaning And Units
BTU	British Thermal Unit
B.O.	Burnout
c_p	Specific Heat Of Propellant Across Test Specimen (BTU/Lb°F)
fps	Feet Per Second
ft	Foot or Feet
°F	Degrees Fahrenheit
h	Heat Transfer Coefficient (BTU/In.^{2}Sec°F)
HDA	High Density Acid (consisting of 56 percent, by weight, of HNO_3 and 44 percent N_2O_4)
h_g	Combustion Gas Film Conductance
I	Current Flow Through Test Specimen (Amperes)
I.D.	Inside Diameter Of Test Specimen (Inches)
in.	Inch or Inches
in.^{2}	Square Inches
K_L	Thermal Conductivity Of A Liquid (BTU/In.^{2}Sec°F)
K_{metal}	Thermal Conductivity Of A Metal (BTU/In.^{2}Sec°F)
kw	Kilowatt
L	Length Of Test Specimen (Inches)
lb	Pound or Pounds
mv	Millivolt
N_2O_4	Nitrogen Tetroxide

LIST OF ABBREVIATIONS AND SYMBOLS (cont)

Symbol or Abbreviation	Description Or Meaning And Units
O.D.	Outside Diameter (Inches)
ppm	Parts Per Million
P_i	Test Specimen Inlet Pressure (Psia)
P_o	Test Specimen Outlet Pressure (Psia)
psia	Pounds Per Square Inch Absolute
psid	Pounds Per Square Inch Differential
P_X	Pressure At Station X Of Test Specimen (Psia)
q	Volumetric Flow Rate (Cubic Feet/Second)
Q/A	Heat Flux (BTU/In.^{2} Sec)
Q_{in}	Energy Transfer Into System (BTU/Sec)
Q_{out}	Energy Transfer Out Of System (BTU/Sec)
r	Inside Radius Of Test Specimen
sec	Second or Seconds
T_B	Bulk Temperature (°F)
T_i	Test Specimen Inlet Temperature (°F)
T_o	Test Specimen Outlet Temperature (°F)
T_s	Tube Surface Temperature (°F)
T_{sat}	Saturation Temperature (°F)
T_W	Tube Inside Wall Temperature (°F)
V	Flow Velocity (Fps)

LIST OF ABBREVIATIONS AND SYMBOLS (cont)

Symbol or Abbreviation	Description Or Meaning And Units
$\dot{W}$	Mass Flow Rate (Lb/Sec)
X	Thermocouple Station (Inches)
Δ	Differential Operator
ΔE	Voltage Drop Across The Specimen (Volts)
ΔT	Temperature Differential
ρ	Density Of Propellant (Lb/Cu. Ft)
μ	Viscosity Of Propellant (Lb/Ft Sec)

1.0 INTRODUCTION

Previous HDA work was conducted by BAC under Lockheed Missiles and Space Company Subcontract to Air Force Contract FO4701-68-C-0235 in 1970 (Reference 1). This program involved Agena Engine fire test investigations with HDA/UDMH and HDA/UDMH + Si propellants. Although satisfactory engine operation was demonstrated the thrust chamber thermal margin could not be defined since the HDA coolant properties were unknown. Further, since a Modified HDA containing PF_5 inhibitor was developed under Task I a need for experimental determination of its coolant properties was required.

Iron contamination of HDA occurs during manufacture and storage and the present procurement specification requires maximum limits of 20 ppm as iron oxide (Fe_2O_3) for procurement and 30 ppm for use. These limits resulted from early Agena engine development fire tests during which thrust chamber overheating occurred. This overheating was attributed to iron contamination of the IRFNA coolant (Reference 2).

The overall objective of this program is to improve the propellants used in the Agena and other propulsion systems. As a result of conducting this task the following specific objectives were achieved:

(1) The heat transfer properties of Standard and Modified HDA were established; and (2) the effect of iron impurity level up to 100 ppm as Fe_2O_3 on heat transfer of Standard and Modified HDA was determined.

2.0 SUMMARY, CONCLUSIONS, AND RECOMMENDATIONS

2.1 Summary

Heat transfer tests were conducted with resistance heated 6061T6 aluminum, 1/8-inch diameter tubes to determine the coolant characteristics of Standard and Modified HDA. The effects of iron impurity level, propellant inlet temperature and simulated engine shutdown were established. Thirty tests were conducted, 15 with each type HDA. Coolant conditions, velocity and pressure, were those characteristic of the Agena thrust chamber which is regeneratively cooled with HDA.

2.2 Conclusions

As a result of performing this work the following conclusions were obtained:

Normal nucleate boiling did not occur with either of the HDA compositions. As the heat flux was increased the tube wall temperature increased much above the saturation temperature of 280°F. Film boiling cooling was apparent up to wall temperatures of about 900°F when tube failure occurred. As the wall temperature increased above 300°F, heat transfer was adversely affected with both HDA compositions at all levels of iron impurity.

Tubes which had previously been operated at wall temperatures above 300°F with shutdown, generally exhibited increased thermal resistance during the subsequent test. For Standard HDA, this effect was observed to vary with iron impurity level, i.e., slight at 30 ppm, nil at 55 and 72 ppm and pronounced at 96 ppm. This effect was observed as an increased thermal resistance which caused generally higher wall temperatures to support a given heat flux. This increased thermal resistance was attributed to scale formed on the inner surface of the tube. Qualitative analysis of the scale from a sectioned tube showed its composition to be inorganic sulfates and nitrates, with aluminum as the major metallic component.

Tests with Modified HDA showed that increased thermal resistance was exhibited at each of the iron impurity levels of 10, 50 and 97 ppm. Tests with tubes which had previously been operated up to near engine conditions and shutdown by venting to simulated altitude conditions generally indicated presence of the increased thermal resistance. Slight scale formation was observed on the sectioned tubes, which chemical analyses showed to be inorganic nitrates, with aluminum as the major metallic component.

Iron impurity level had no effect on the forced convection heat transfer coefficients which were derived from initial tube tests.

Comparison of results showed that the Modified HDA exhibited about 10% lower forced convection heat transfer coefficients but somewhat higher heat flux at tube destruction than Standard HDA.

The effect of propellant temperature followed the expected trend of increasing heat transfer coefficient with increased bulk temperature.

Thermal analysis of the Agena thrust chamber using the results from the investigation indicate that adequate thermal margin exists for the most severe coolant side conditions.

2.3 Recommendations

Based on results from this investigation, it is recommended that the present HDA specification limits for iron impurity be relaxed. Agena thrust chamber fire tests are recommended to demonstrate operation with higher iron impurity level, prior to HDA procurement and use limits specification changes.

3.0 TECHNICAL DISCUSSION

3.1 Test Plan

Thirty tests were planned to establish the effects of soluble iron impurity on the heat transfer characteristics of HDA. Effects of the impurity level were determined with both Standard and Modified HDA at two levels of bulk inlet temperature. Composition of Standard and Modified HDA is included in Table I. In addition, simulated shutdown under altitude conditions was evaluated. The following test variables and associated levels were investigated:

Percent Iron Impurity	3 levels	20 ppm 60 ppm 100 ppm
Type HDA	2 levels	Standard Modified
Type Test	2 levels	W/O Shutdown W/Shutdown
Bulk Inlet Temperature	2 levels	32°F 90°F

The minimum number of tests necessary to conduct a statistically complete test program is $2^3 \times 3 = 24$. Furthermore, simulated shutdowns require two tests which increases the total number of tests to thirty-six.

These thirty-six tests can, under certain assumptions, be reduced by conducting a partial factorial test program. Therefore, assuming that the second order interaction among the variables with two levels are negligible, and noting that the effects of percent impurity are of primary importance, it was decided to fractionalize with respect to only the variables with two levels. The resultant test plan was one half replicate of the complete 2^3 experiment, with the following test series conducted at each impurity level.

Bulk Temperature	HDA Type	Test Type
32°	STD	W/O Shutdown
90°	STD	W/Shutdown
90°	STD	W/O Shutdown
32°	MOD	W/Shutdown
32°	MOD	W/O Shutdown
90°	MOD	W/O Shutdown

A matrix consisting of 18 tests as shown in Table II was planned for initial evaluation. This left 12 tests available to further define the relationship between the response variables and the impurity level.

3.2 Test Specimen

Each test specimen (Figure 1) was constructed from a 10.7 inch seamed tubing section of 6061T6 aluminum of 1/8-inch nominal tube diameter. The actual outside diameter of the tube varied between 0.1258 and 0.1265 inches with a wall thickness of 0.020 ± 0.002 inch. The 10.7 inch section allowed six inches for the heated section, four inches for the two electrodes, and 0.7 inches for attachment to the upstream and downstream adapter fittings.

The heated length of 6 inches was selected for two reasons:

(1) It provided sufficient electrical resistance to generate a heat flux well beyond the expected maximum burnout heat flux for the test program.

(2) It provided a convenient length with enough room to attach five surface temperature thermocouples.

Aluminum sleeves were joined to the 6061T6 aluminum test sections by an interference fit. This allowed for the attachment of large copper bus bar clamps for electrical power input. Because of the very small resistance associated with this bus bar clamp technique, almost all the resistance and thus the temperature rise, occurred in the six inch test section.

Surface temperature thermocouples were made by tightly twisting No. 28 gauge chromel-alumel wire together and forming a junction bead by arc welding, using an inert gas and a non-consumable tungsten electrode. The thermocouple junction bead was made as small and as smooth as possible and then turned to the inside to contact the tube surface. The thermocouples were electrically insulated from the tube surface by an initial uniform ceramic coating of aluminum oxide which was 0.005 ± 0.001 inch thick. A support was installed across the pressure fittings approximately one inch from the top as shown in Figure 2, and the individual leads were formed around the tube, pulled taut and secured to the support. The outer insulation was pulled down and a recheck made of each thermocouple bead to assure contact to the initial coating. A second coating of aluminum oxide approximately 0.030 inches thick, was then applied over the entire length of the test section of the tube to securely fasten the surface thermocouples as shown in Figure 3.

3.3 Test Apparatus

Power was provided by four 28 volt dc - 750 ampere, compound-wound Hobart motor generators. These units were connected in an equalizer bus connection in the positive leg, which tied their series fields in parallel. A contactor rated at

1000 amps dc, complete with arc chute and blowout coil was installed in the negative leg of each machine, so that it could be switched on-line individually. The field of each generator was separately excited by a 0-72 vdc supply, resulting in a saturation no-load terminal voltage of 50 vdc. Generator bus bars and cable were sized for 1000 amps per machine. The entire system was wired for a capacity of 4000 amps.

When the tube failed the generators were shut down, the upstream and downstream propellant valves were closed and a CO_2 fire extinguishing system was automatically turned on. In all cases the termination of the test was well controlled with no test stand damage.

Shutdown simulation tests at 70% of burnout were terminated by automatically switching the generator contactors off, closing the upstream propellant valve and energizing a three-way valve. This ducted the downstream section of the test specimen to a vacuum tank, all in a timed sequence (see Figure 4).

The power source characteristics map shown in Figure 5 was constructed to depict the voltage and current values expected. Only aluminum tubes with 0.020 inch wall thickness were available, although 0.015 inch wall thickness tubes were sought. Superimposed on the map are lines of constant heat flux covering the expected range for the HDA.

The propellant supply system is shown schematically in Figure 6. The supply tank and receiver tank each have a capacity of 100 gallons and can be pressurized to 1200 psia. For this program the supply tank contained 90 gallons of propellant which allowed test durations of up to 60 minutes for an 1/8 inch tube at a flow velocity of 75 feet per second. Both the supply and receiver tanks were pressurized with a regulated gaseous nitrogen source to obtain the required 750 psia operating pressure at the test specimen.

Propellant was conditioned to the required inlet temperatures by a system consisting primarily of a circulation pump, and a steam heat exchanger for hot conditioning or a CO_2 cooled brine exchange for cold conditioning. It is a closed loop system, circulating the propellant from the supply tank only, and can provide uniform propellant temperatures over the entire range of 30° to 200°F. During the test the propellant conditioning system was isolated from the supply tank.

A 1/2 inch diameter line carried propellant to the test section. Flow was controlled by two parallel valves (one for coarse adjustments and one for fine adjustments) which were located downstream of the test section. The test section could be isolated from the supply and receiver system by upstream and downstream pneumatic operated valves. Under normal operating conditions, flow through the test specimen was remotely controlled by these valves. Whenever a rapid drop in pressure occurred (as is the case at tube destruction) a pressure switch automatically closed these valves, isolating the test section. The receiver tank was vented to sea level atmospheric conditions during all tests except those designed to determine the effect of simulated altitude shutdowns. Altitude simulation capability of approximately 100,000 feet was provided by an aspirator vacuum tank and cold trap connected to the three-way type propellant valve located immediately downstream of the test section.

3.4 Test Instrumentation

Standard instrumentation provided the capability of recording propellant flow rate, supply and receiver tank pressures, inlet and outlet pressure and temperature, surface temperatures, and the current flow and voltage drop.

Pressure measurements were made with Taber Teledyne (PSIA) transducers and Statham (PSID) transducers. Transducers used to measure the inlet and outlet pressures were electrically isolated from the heated test section by special insulation blocks. The demonstrated measurement uncertainty for this type of transducer is ±0.7% (three sigma) of nominal output.

Propellant temperatures were measured using probe type chromel-alumel ungrounded thermocouples, which are imbedded in a mineral insulation and protected from the propellants by a stainless steel sheath. The demonstrated measurement uncertainty for these thermocouple probes is ±2.0°F of nominal temperature.

Surface temperatures of the test tubes were measured with thermocouples made from No. 28 gauge chromel-alumel wire with an asbestos/glass fiber insulation. Accuracy of these thermocouples is rated at ±4.0°F up to 530°F and ±0.75% from 530°F to 1400°F. All of the thermocouples, four propellant and five surface temperatures, were referenced to 150°F using a Pace Reference Junction Box.

The power delivered to the test section was determined by measuring the current flowing in the circuit and the total voltage drop across the heated section of the tube. Current was measured with a shunt calibrated to generate 50 mv at 2000 amps. Voltage was measured directly across the test section by wires attached to the bus-bars. To obtain a millivolt output, the measured voltage was divided by a calibrated circuit.

Redundant Fischer-Porter turbine-type flowmeters were used to measure propellant flow rates. Prior to the initiation of the test program the flowmeters and their installation line sets were calibrated as a unit in water. At least two calibrations, over the expected region of operation, were conducted on each flowmeter set and an average sensitivity derived for test data reduction. Measurement uncertainty associated with this type of flowmeter has been demonstrated to be approximately ±1.0%.

Millivolt outputs of the transducers, the current level and voltage drop across the test specimen were patched to signal conditioners and recorded on a Brush Recorder, with an accuracy of ±3% of full scale; A CEC Oscillograph, with an accuracy of less than ±5% over the range of the galvanometer used; and on a Beckman Model 210 Data Acquisition System, with an accuracy of ±0.1% for 20 millivolt full scale input. The Beckman 210 data acquisition system converts the conditioned millivolt outputs of the various transducers and measured devices to a digital data bit and records the data on magnetic tape in a format suitable for data reduction on an IBM 360 Model 44 computer.

3.5 Test Procedure

General procedure for conducting a test was to first condition the propellant to the desired inlet temperature by circulating from the supply tank with an appropriate heat exchanger. The test specimen was installed in the test stand, see Figures 7 and 8, pressure tested and an instrumentation check made. The next step was to pressurize the propellant system to the flow control valves by means of the gaseous nitrogen regulator. Flow control valves were then adjusted to obtain the proper inlet velocity and operating pressure at the test specimen. Once the desired propellant system conditions were obtained, a 10 second data file of the test parameters, such as supply pressure, flow rate, inlet and outlet temperature and pressure, and receiver tank pressure was recorded on magnetic tape.

Power was then applied to the test specimen in predetermined increments. Once steady-state was attained at each increment, as evidenced by a visual recording of the test specimen outside wall thermocouples, a 10 second data file of all pertinent parameters was recorded on magnetic tape. This procedure was followed until either 70% of the anticipated burnout point or the anticipated simulated shutdown point was achieved, depending on the nature of the test being conducted. The data recorders were then turned on and continuous recording of data was made as power was incrementally applied until automatic shutdown occurred (in the case of burnout). In the case of simulating an altitude shutdown the test engineer manually terminated the test from the control panel.

3.6 Data Reduction

Test data were obtained from the electrical output of the various pressure transducers, flowmeters and thermocouples. The outputs were converted to and recorded as digital data on a magnetic tape. These data were then used as inputs to a series of assembler and Fortran language programs which performed the calculations necessary to produce engineering units and data. The physical properties of the tube materials and propellants were inputs to these programs. These data were obtained from References 3 and 4.

The following describes the engineering rationale and resultant equations which were programmed for the computer.

The heat flux into the liquid at any point is given by the following equation:

$$Q/A = \frac{(0.000948)\ (\Delta E)\ (I)}{(\pi)\ (I.D.)\ (L)} \quad \frac{BTU}{Sec\text{-}in.^2}$$

Heat flux was treated as a constant along the length of the tube.

Bulk temperature at any station is given by the following equation:

$$T_B = T_i + (T_o - T_i)\frac{X}{L} \quad °F$$

This assumes that no significant change in temperature occurs outside the heated section, and that the temperature variation along the length of the tube is linear.

The equation for local static pressure is similar to the equation for bulk temperature. However, it is assumed that pressure drops linearly between the two pressure taps which are placed at either end of the 11-inch test section and a single phase flow exists. The pressure is therefore given by the following equation:

$$P = P_i - (P_i - P_o)\frac{2.5 + X}{11}$$

Inside wall temperature at each thermocouple station along the heated section of the tube was calculated from the thermal conductivity of the tube material and the measured power input, surface temperature, and tube dimensions, i.e.

$$K_{metal} = A + BT_s$$

$$T_W = \frac{-A + \left(A^2 + 2B.\left\{AT_s + \frac{B}{2}T_s^2 - Q/A.\left[\frac{I.D.}{1-\left(\frac{I.D.}{O.D.}\right)^2}.\ln\left(\frac{O.D.}{I.D.}\right) - \frac{I.D.}{4}\right]\right\}\right)^{1/2}}{B}$$

Where A and B are the coefficients of the appropriate thermal conductivity relationship.

Energy transfer into and out of the system is given by the following equations:

$$Q_{in} = 0.000948\ (\Delta E)\ (I)\ \frac{BTU}{sec}$$

$$Q_{out} = \dot{W}\,\bar{C}_p\left(T_o - T_i - (T_o - T_i)_{Q/A=0}\right)$$

All of the electrical energy released into the system is assumed to be converted to enthalpy increase of the fuel. Heat losses due to convection and radiation have been calculated and found to be negligible. Change in the kinetic energy of the fluid as it passes through the system is negligible. The $(T_o - T_i)_{Q/A=0}$ term is included to account for frictional effects and thermocouple errors which are present before power is applied.

Flow rate used in the equation above was derived from the measured volumetric flow rates:

$$\dot{W} = \rho \cdot q$$

Where q is the measured volumetric flow rate, and ρ, is the propellant density.

The heat transfer coefficient can be calculated at any station by applying the equation shown below.

$$h = Q/A \ (T_w - T_B)$$

Flow velocity is calculated by applying the simple one-dimensional continuity equation:

$$V = W \ (\rho) \frac{(I.D.^2)}{(4x144)} \ (\pi)$$

where I.D. is the inside diameter of the appropriate test specimen.

The computer was also programmed to calculate the following dimensionless correlation parameters with fluid properties evaluated at local bulk temperatures and estimated mean film temperatures.

Nusselt Number	$Nu = \frac{(h)\ (I.D.)}{K_L}$
Reynolds Number	$Re = \frac{(I.D.)\ (V)\ (\rho)}{\mu}$
Prandtl Number	$Pr = \frac{(C_p)\ (\mu)}{K_L}$

These parameters were utilized to monitor test results.

3.7 Description of the Heat Transfer Process

A graphic illustration of the heat transfer process for forced convection turbulent flow of normal fluids is shown in Figure 9. With reference to this figure, the heat transfer process may be explained as follows:

a. The boundary layer characteristics for the nonboiling condition are shown. The heat is transferred through three layers.

Layers	Mode of Heat Transfer
Laminar Sub-layer	Conduction
Buffer Layer	Conduction and Eddy Currents
Turbulent Layer	Eddy Currents

In this region the thermal resistance to heat transfer remains constant for a given flow rate, geometric configuration and type of fluid. The driving force is the temperature difference between the heated surface and coolant temperature.

b. If the heat transfer rate is sufficiently high, the heated surface temperature may exceed the saturation temperature of the coolant, and nucleate boiling will occur at the heated surface. The agitation of the boundary layer caused by these fast moving bubbles, decrease the thermal resistance to heat transfer to such an extent that it is possible to obtain increased heat transfer rates with no change in heated surface temperature. As the rate of heat transfer increases, the bubble population increases to such a point that a vapor layer covers the heated surface. From this point the heat transfer process may proceed by two means.

c. If the thermal resistance offered by the gas film is low enough, stabilized film boiling will occur. The heat will be transferred across this vapor film into the liquid. Stabilized film boiling will usually occur at high coolant velocities and at pressures above the coolant's critical pressure. Failure of the heated surface occurs when the temperature exceeds the melting point or the working pressure exceeds the stress limit of the material at this higher temperature.

d. If the thermal resistance of the vapor film is great enough, the temperature of the heated surface will rise to the melting point of the material and burnout will occur.

3.8 Test Results

Shown in Figure 10 is the heat flux versus wall temperature for Test 1199 which typifies the general trend of results obtained with the HDA. It can be seen that wall temperature increases with heat flux to values much in excess of saturation. Normal nucleate boiling did not occur when the wall temperature increased above the saturation temperature of 280°F. An audible oscillation was observed at wall temperatures in excess of about 400°F. The tube was apparently cooled by film boiling and the oscillation was attributed to two phase flow. Also, surface temperatures were non-uniform with abnormal temperature gradients indicated along the tube length in this film boiling mode. These temperature gradients increased with heat flux until tube burnout occurred. Measured and derived data for Test 1139 are included in Table III which shows tube wall inner wall temperatures of 908°F near the inlet (Station 1) and 445°F near the outlet (Station 5) at a heat flux (Q/A of 1.58 BTU/in.^{2} sec. The average inside wall temperature of this data point was 637°F.

This test was a repeat of the initial test conducted with a coolant inlet temperature of 32°F. This test condition always resulted in tube wall temperature maximums and tube destruction near the inlet end. Tests at 50°F inlet resulted in tube wall temperature maximums and tube destruction near the outlet end. Because of the abnormal results obtained from the initial test some additional verification tests were conducted including one with CRES 347 tube material.

Results from the CRES 347 tube testing were consistent with the 6061 aluminum material testing except that the former exhibited much higher heat flux at tube destruction. This was attributed to the higher temperature capability of the CRES 347. Wall temperatures in the range of 1800°F were indicated and the tube was observed to glow during this test. A summary of heat transfer test results is presented in Table IV.

3.8.1 Effect of Iron Impurity Level

In accordance with the test matrix the first test series was conducted with Standard HDA containing 30 ppm iron impurity as Fe_2O_3. This impurity level was somewhat higher than the 20 ppm level originally planned, however, it was considered satisfactory for use since it conformed to the maximum iron concentration use limits allowed in MIL-P-7254F. Tests with Standard HDA were then conducted at 96, 55 and 72 ppm. Impurity concentration was controlled by iron nitrate addition or dilution techniques. Results from these tests are presented in Figures 11, 12, 13, and 14 which show the heat flux versus wall temperature characteristics obtained. Each of these figures include the shutdown test during which the tube was operated up to the heat flux condition corresponding to that of the Agena thrust chamber throat station and then subjected to a simulated altitude shutdown after which the same tube was then operated to burnout. As the wall temperature increased above 300°F heat transfer was adversely affected with both HDA compositions at all levels of iron impurity.

Tubes which had previously been operated at wall temperatures above 300°F with shutdown, generally exhibited increased thermal resistance during the subsequent test. For Standard HDA this effect was observed to vary with iron impurity level, i. e., slight at 30 ppm, nil at 55 and 72 ppm and pronounced at 96 ppm.

This effect was observed as a reduced heat transfer coefficient or an increase in thermal resistance which is indicated by the generally higher wall temperatures required to support a given heat flux. This increased thermal resistance is apparently caused by scale formed on tube inner surface. Inspection of Figures 11-14 indicates that the scale appears to form, as reflected by the change in slope, at heat flux values above 3.0 BTU/in.^{2} sec with corresponding wall temperatures above 300°F. The tube from Test 1207 which was sectioned for observation and analysis, showed a tan gel over a brown stain. Qualitative analyses by emission spectroscopy and infrared, revealed that the scale was composed of inorganic sulfates and nitrates with aluminum as the major metallic component.

Similar tests were then conducted with Modified HDA (0.55% PF_5) containing iron contaminant levels of 10, 50 and 97 ppm.

The 10 ppm level for the initial series was the iron measured upon chemical analysis after blending the Modified HDA in the test cell tank. Subsequently, the impurity level was adjusted by adding iron nitrate.

Shutdown tests were conducted with a propellant inlet temperature of 32°F, and the 10 ppm tests were repeated at a 90°F inlet temperature. Results presented in Figures 15, 16, and 17 show that the increased thermal resistance was indicated at each of the contaminant levels investigated. However, the variation between the initial and burnout test was somewhat different than that observed with Standard HDA. It was observed from these tests that the effect was greatest at 50 ppm with less degradation at 97 ppm. No cause for this could be established, however, it should be noted that chemical analyses indicated the total solids of the Modified HDA increased from 0.026% initially to 0.120% following Test 1223, and finally to 0.140% at the conclusion of the program. It is possible the higher solids which indicates higher concentration of aluminum nitrate altered the scale composition formed during tests subsequent to Test 1223.

Tubes from Tests 1223 and 1226 were sectioned for observation and analysis. It should be noted that each of these tubes was inerted prior to sectioning with methylene chloride while the tube from test 1207 was inerted with water. This inerting fluid was selected because it has little or no dissolving effect on the scale deposit. Results of the chemical analyses which showed there was less deposit when PF_5 was used as inhibitor are included below. The major metallic component was aluminum. Infrared showed mostly anhydrous inorganic nitrates. Hydrates and sulfates were also discernible in the deposit formed from Standard HDA. Rather than attributing the variance in the analysis results to a different reaction or material, it was concluded that the water inerting used on Test 1207 formed the hydrates and removed most of the nitrates.

TUBE ANALYSIS RESULTS

Test	Appearance Of Tube	Inhibitor	Spectroscopic	Infrared
X1-1207	Moderate coat, tan gel over brown film	HF	Al > Fe, Cu	Hydrated Sulfates Hydrated Nitrates
X1-1223	Trace of white salt	PF_5	Al > Fe, Cu	Anhydrous Inorganic Nitrates
X1-1226	Small amount of white salt over brown stain	PF_5	Al > Fe, Ni, Cu	Anhydrous Inorganic Nitrates

3.8.2 Effect Of Inlet Temperature

Temperature effects were included by conducting the heat transfer tests at 32 and 90°F. It was previously mentioned that all of the burnout tests at 32°F inlet temperature exhibited maximum tube wall temperatures at Station 1, near the inlet. Tests at 90°F inlet temperature indicated a maximum tube wall temperature at Station 5, near the tube outlet. These effects were as predicted by calculation of the forced convection heat transfer coefficient h_L according to the classical correlation - $h_L = 0.0265 \left(\frac{DV\rho}{\mu}\right)^{0.8} \left(\frac{c_p \mu}{k}\right)^{0.4} \frac{k}{D}$.

The h_L is a function of temperature since the coolant properties vary with temperature. This temperature effect was calculated to show the variation of h_L over the inlet temperature range evaluated using the properties of Reference 5 as shown below:

		HDA Properties	
		32°F	90°F
Density	g/cc	1.677	1.612
Viscosity,	Centipoise	4.95	1.88
Specific Heat, c_p	BTU/Lb °F	0.446	0.446
Thermal Conductivity, K	BTU/Hr Ft °F	0.189	0.184

Substituting in the h_L equation:

$$\frac{h_L\ 90}{h_L\ 32} = \left(\frac{DV \frac{1.612}{1.88}}{DV \frac{1.677}{4.95}}\right)^{0.8} \left(\frac{c_p \frac{1.88}{0.184}}{c_p \frac{4.95}{0.189}}\right)^{0.4} \frac{\frac{.189}{D}}{\frac{.184}{D}}$$

$$= (2.535)^{0.8} \quad (0.391)^{0.4} \quad 1.03$$

$$\frac{h_L\ 90}{h_L\ 32} = 1.495$$

Therefore, the h_L at 90°F is shown to be 50 percent greater than the value obtained at 32°F. The lower h_L at 32°F results in higher wall temperature to support a given heat flux.

Actual forced convection heat transfer coefficients derived from tests of this investigation are presented in Table IV and graphically in Figure 18. Data shown in this figure were normalized to 75 ft/sec inlet velocity. The data follows the predicted trend but the values were generally greater.

3.8.3 Effect Of Velocity

The final three tests were conducted at 30 ft/sec inlet velocity corresponding to Agena thrust chamber section conditions. Results shown in Figure 19 and Table IV show both lower forced convection heat transfer coefficient and heat flux at tube destruction than obtained at 75 ft/sec inlet velocity.

3.8.4 Analysis Of Test Results

A regression analysis of available data from the heated tube test program was conducted to determine the sensitivity of the heat transfer coefficient to various test variables. The variables considered in the analysis were:

Propellant (Standard or Modified HDA)
Iron Impurity Level
Bulk Temperature

Non-linear influences of bulk temperature were also considered. Of the data available three tests were rejected as outliers, runs 1201X-1 (Station 5), 1212X-1 (Station 1) and 1222X-1 (Station 1). However, with the exception of the form of the regression equation obtained, the results concerning the statistical significance of each variable would have been essentially the same even if all the data had been used.

The following results were obtained:

a. The type of propellant used does seem to influence the value of the heat transfer coefficient. Use of Modified HDA results in a decrease in the heat transfer coefficient of about 10%, 0.001 BTU/in.^{2}-sec °F.

b. Over the range tested the iron impurity level has no effect upon the heat transfer coefficient.

c. Bulk temperature has a strong non-linear influence upon the heat transfer coefficient.

On the assumption that the required function should be monotonic a fit of the form $h = \quad T^B$ was established. The resultant expression plotted was given by:

$$h_L = 0.00425\ T^{0.3178}$$

3.9 Application To Agena Thrust Chamber

Peak heat flux of the Agena nozzle at the geometric throat was established based on previous water cooled fire tests with HDA/UDMH + SO. This is the gas side heating rate imposed across a unit nozzle surface area which differs from the heat flux of the heated tubes used in this program and the coolant passages of the thrust chamber. Since the coolant passage is non-uniformly heated with most of the heat flux imposed on that part of the circumference exposed to the gas side, a two dimensional analysis is required to establish heat flux rates and temperature distribution. An analysis was conducted to assess the effect of the experimental results from this program on the Agena thrust chamber thermal conditions. Allowance was made for coolant side scale formation which occurred on most tests at wall temperatures above 300°F by utilizing two values of coolant characteristic as shown in Figure 20.

The chamber throat station wall element is presented in Figure 21 which also includes coolant bulk and gas side conditions, and resulting temperature distributions. A maximum gas side wall temperature of 501°F, which is safely below the maximum design allowable value of 750°F results. Assessment of margin based on peak nucleate boiling heat flux was precluded since HDA exhibited no nucleate boiling character.

4.0 REFERENCES

1. Bell Aerospace Company, Model 8096 Maximum Density Acid Definition Program, Volume I, Bell Aerospace Report No. 8096-910082, September 1970.

2. J. H. Wolf and J. R. Flanagan, Iron Solids Content in Nitric Acid, Bell Aerospace Memo 943:61:0511-1-JHW/JRF, May 1961.

3. Private Communication R. C. Simon to D. J. Alverson, Battelle Memorial Institute, Defense Metals Information Center, Properties of 6061T6 Aluminum, September 1967.

4. R. D. Kalp, Physical Properties of Maximum Density Fuming Nitric Acid (HDA), Bell Aerospace Memo 949:72:0918-1:RDK, September 1972.

5. C. J. Hoffman, High Density Acid (HDA) Physical Properties Handbook, Lockheed Missiles and Space Company, LMSC/D153518, May 1972.

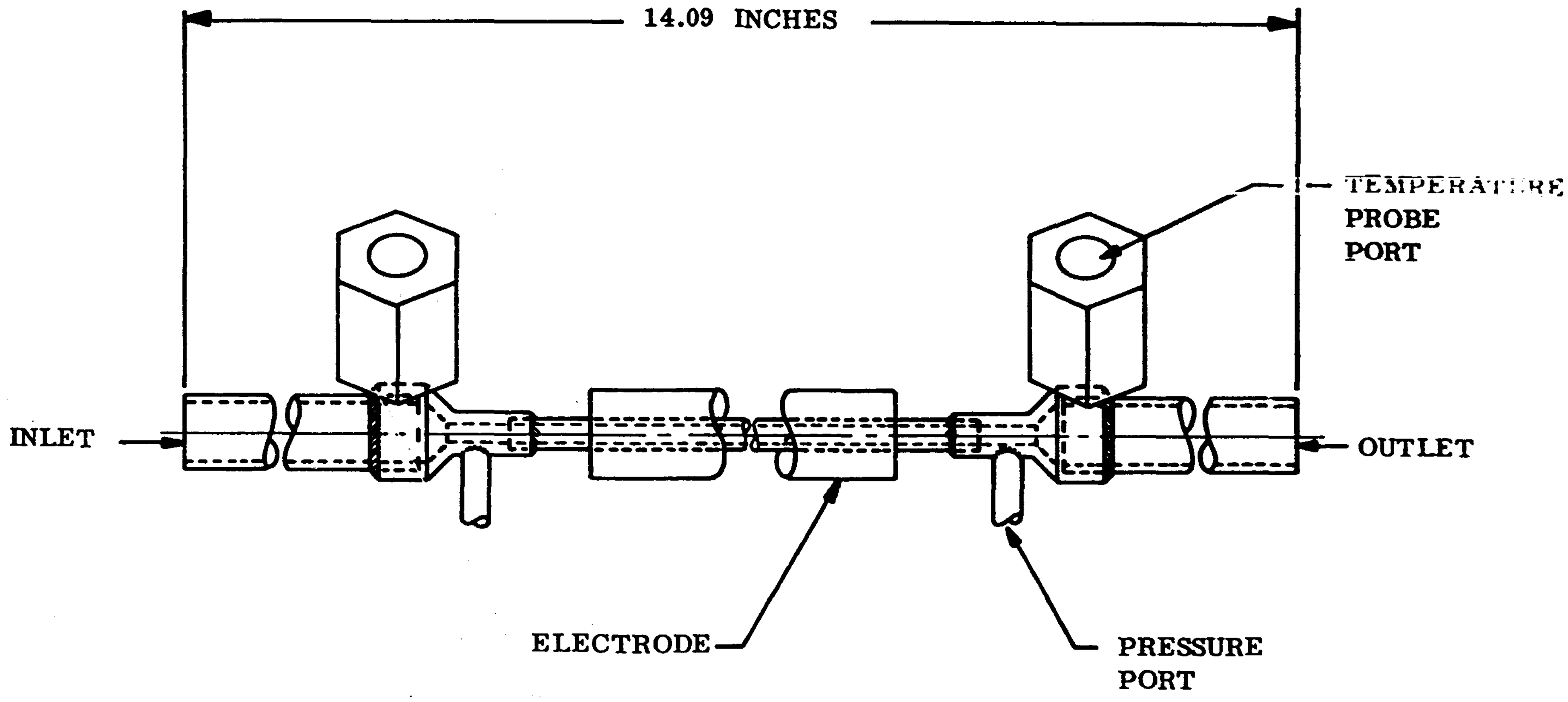

Figure 1. Tube Test Specimen Assembly

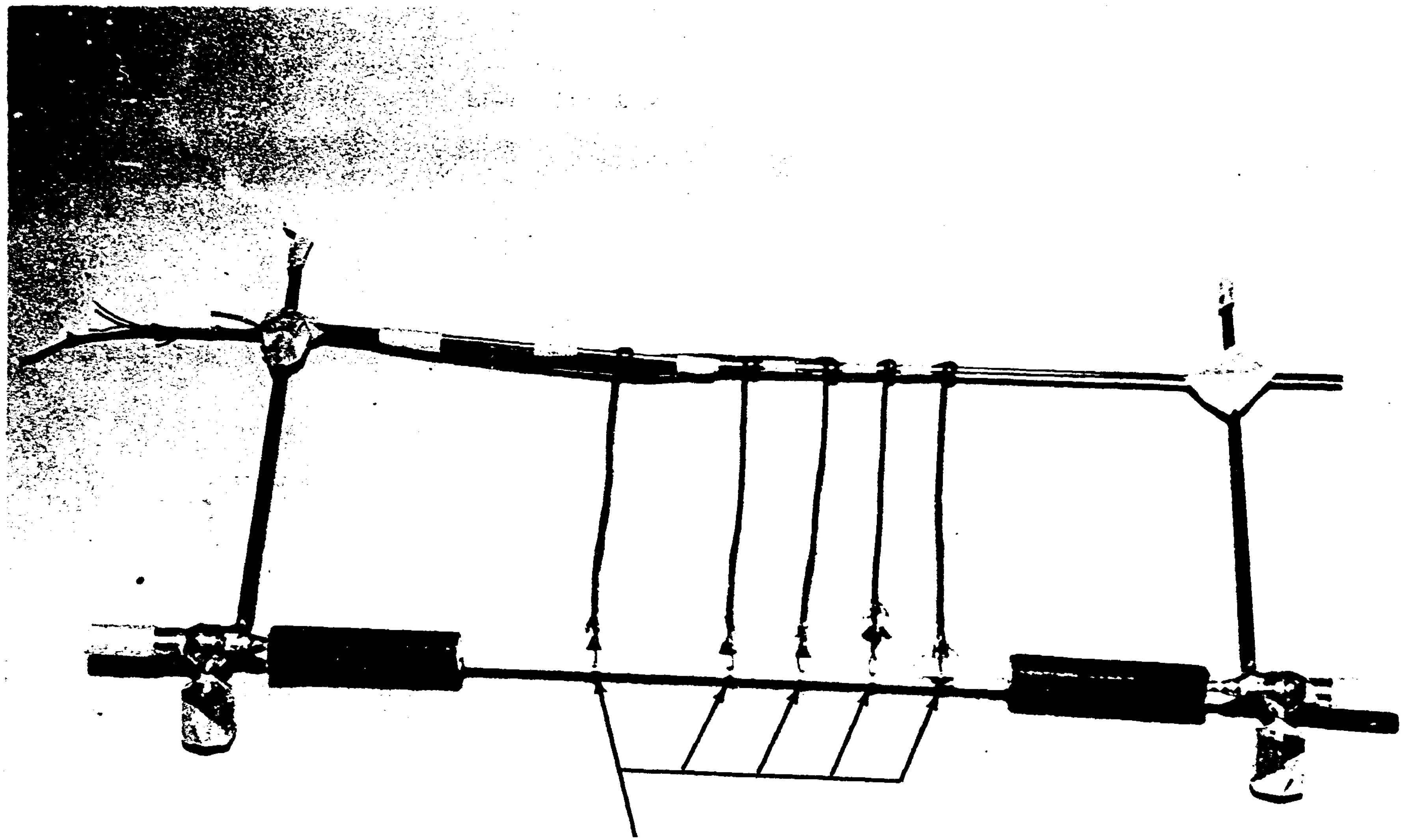

Figure 2. Heat Transfer Tube Specimen Prior To Final Flame Spray

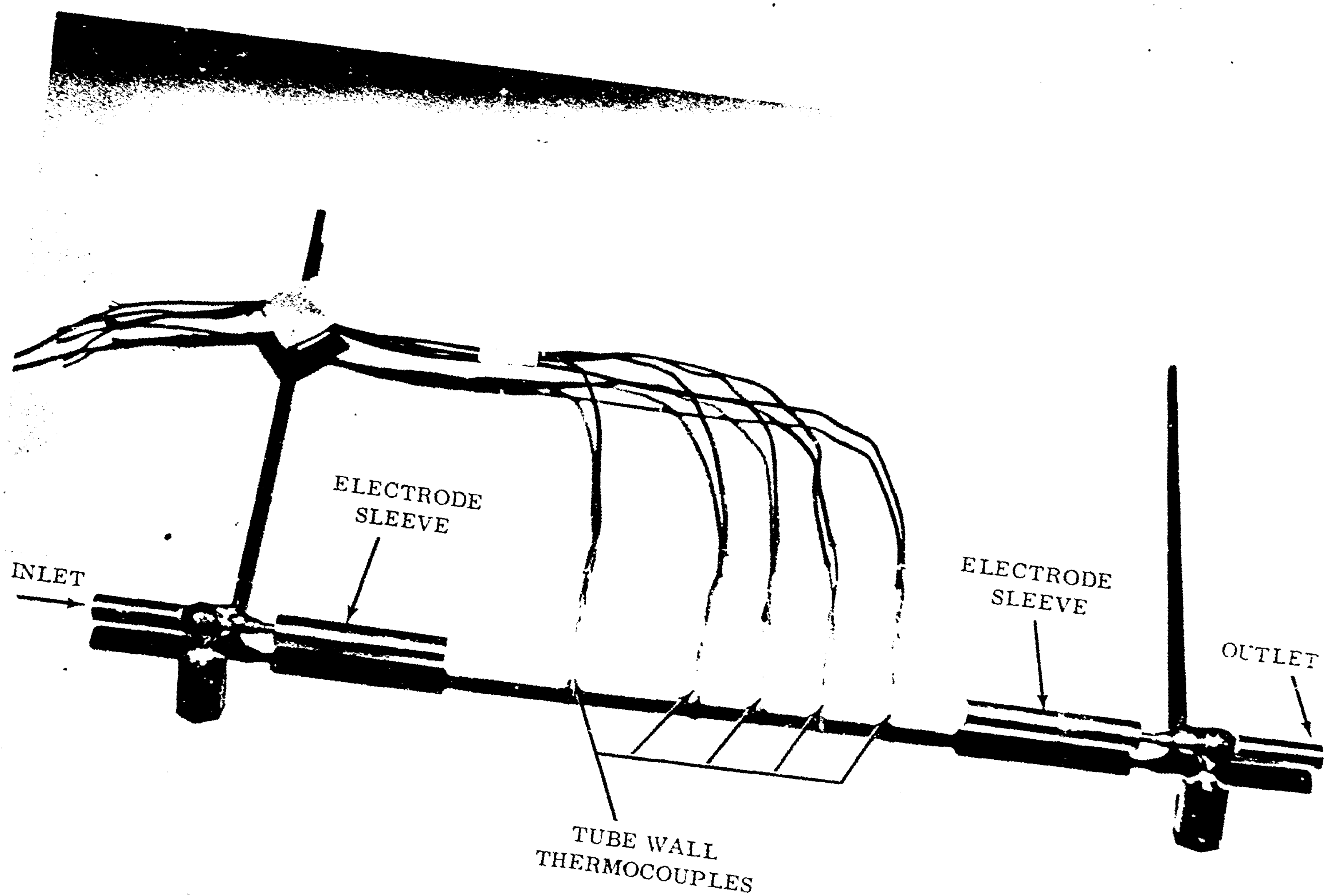

Figure 3. Completed Heat Transfer Tube Specimen

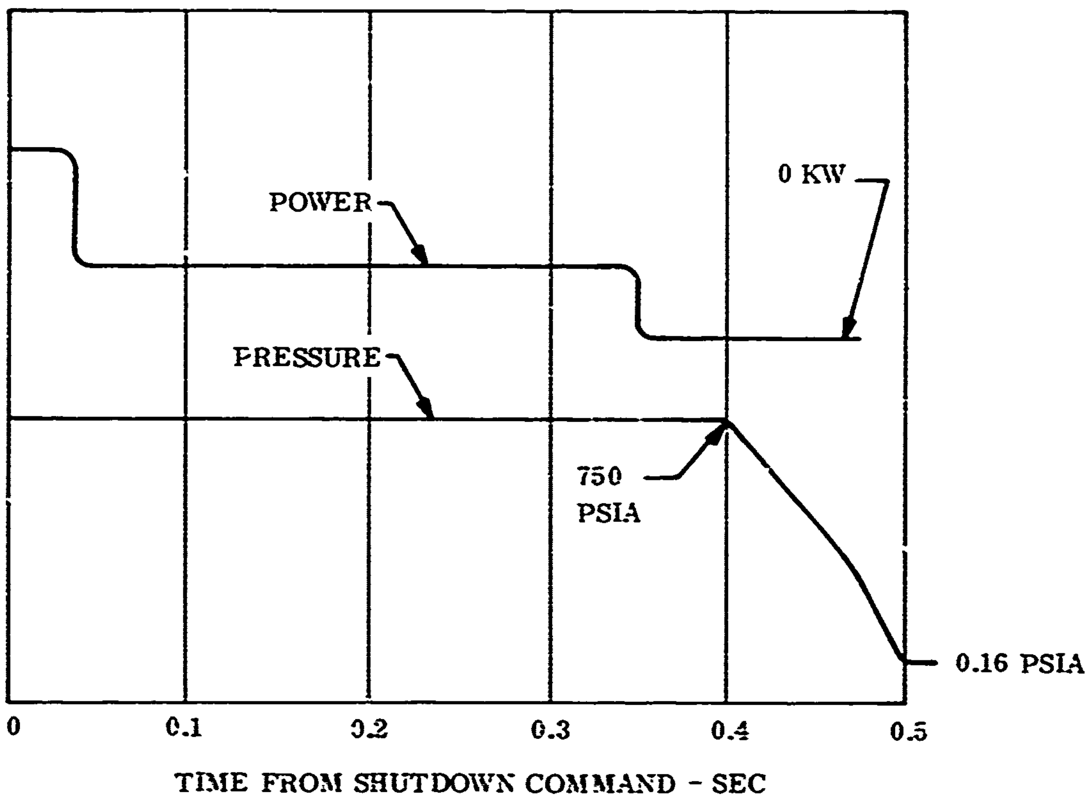

Figure 4. Shutdown Simulation Test Sequence

NOTES: 1. TUBE LENGTH = 6.0 IN.
WALL THICKNESS = 0.015 IN.
UNLESS OTHERWISE SPECIFIED

2 MAXIMUM APPARATUS CURRENT CAPABILITY
3 WALL THICKNESS = 0.020 IN.
4 BTU/IN.^{2} SEC

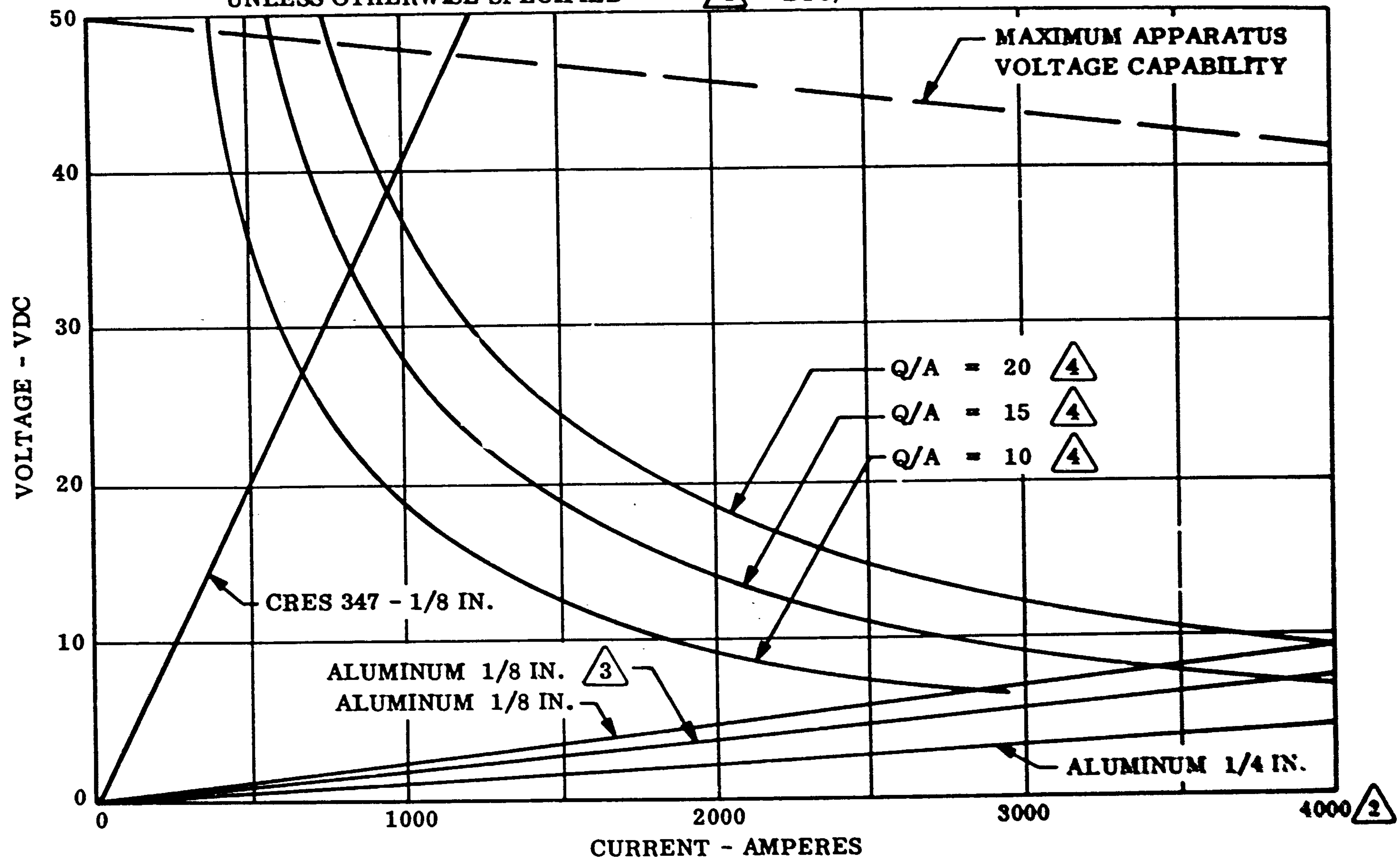

Figure 5. Heat Transfer Test Apparatus Characteristics

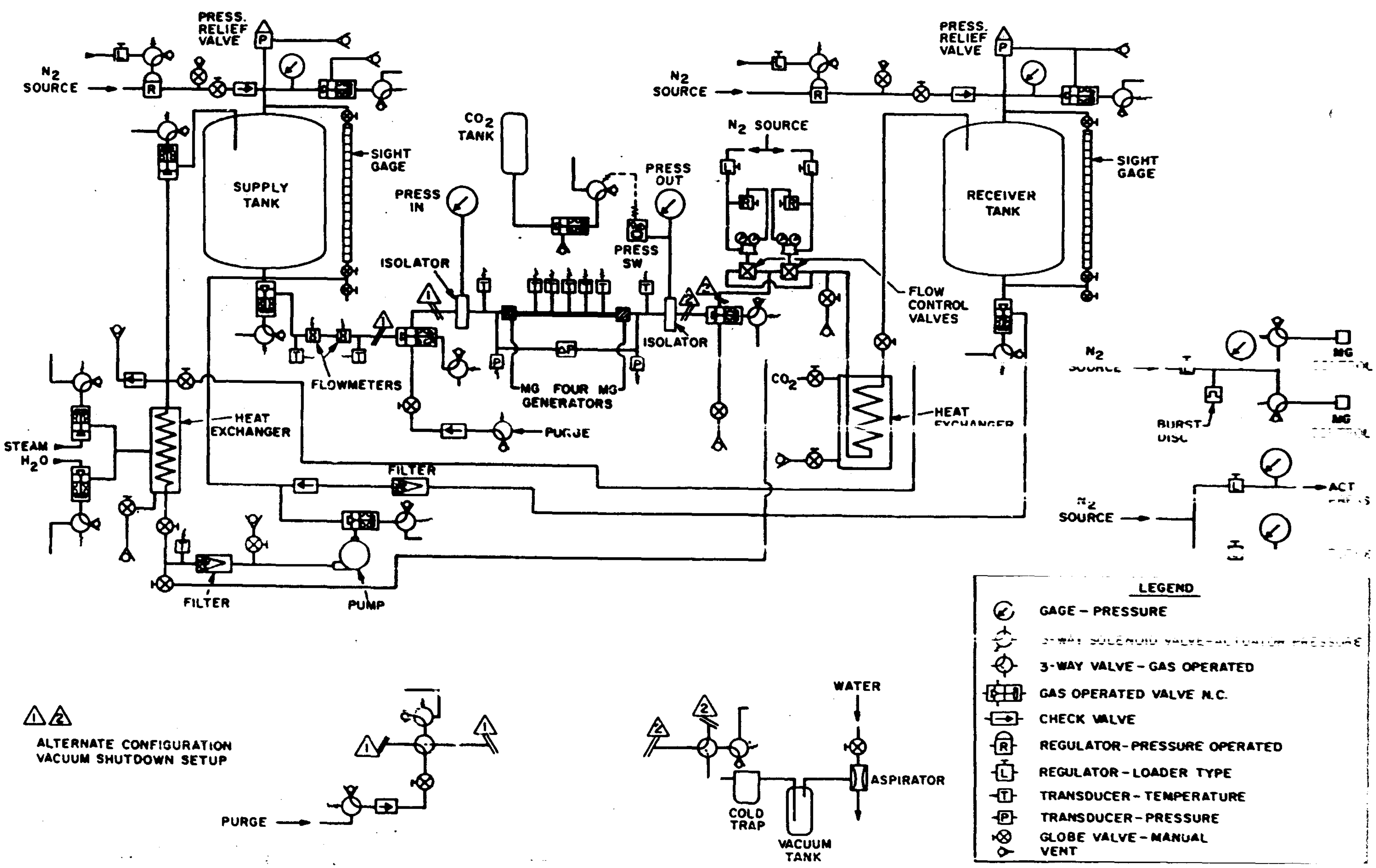

Figure 6. Forced Convection Heat Transfer Test Cell No. X-1 Schematic

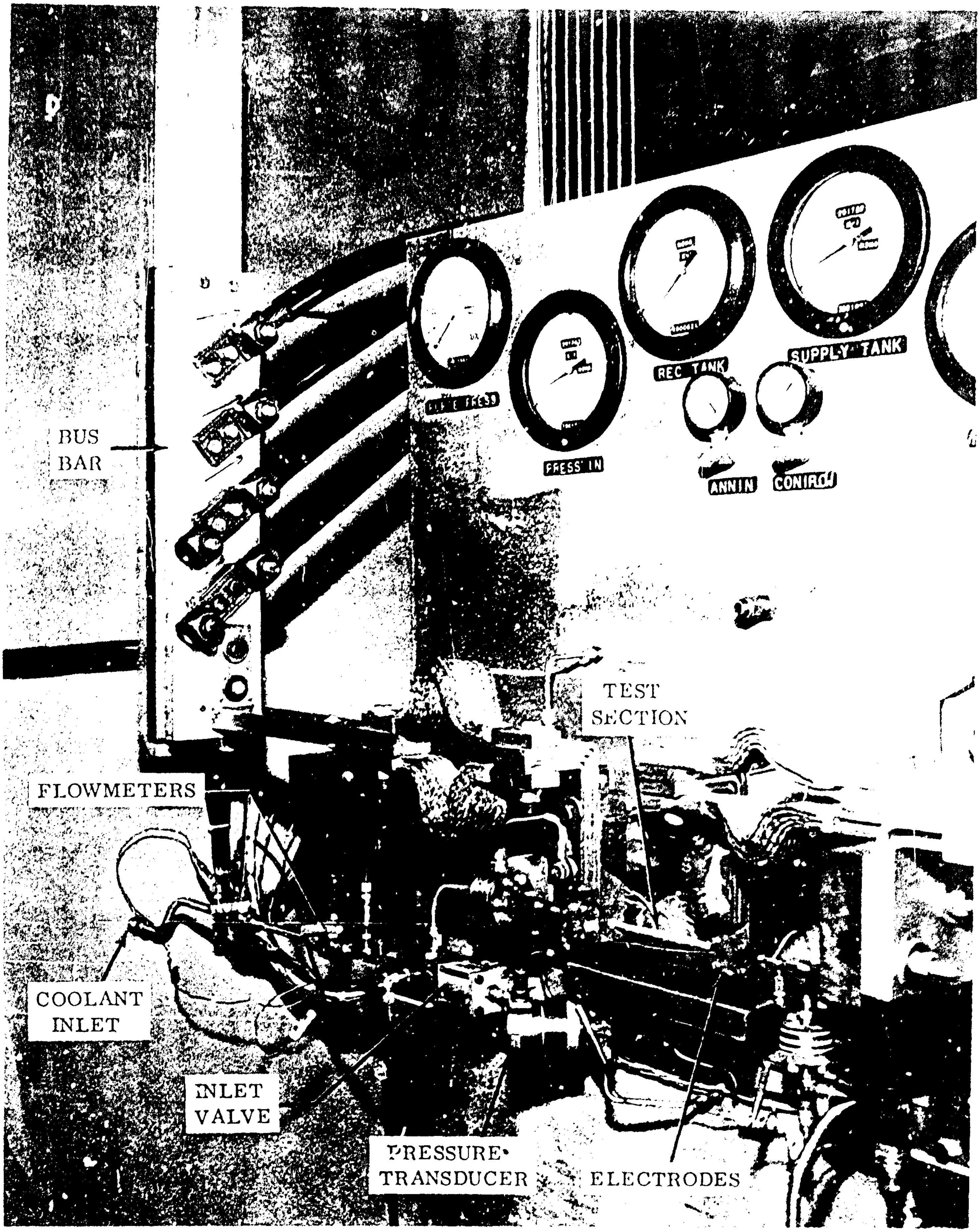

Figure 7. Test Apparatus - Left Side View

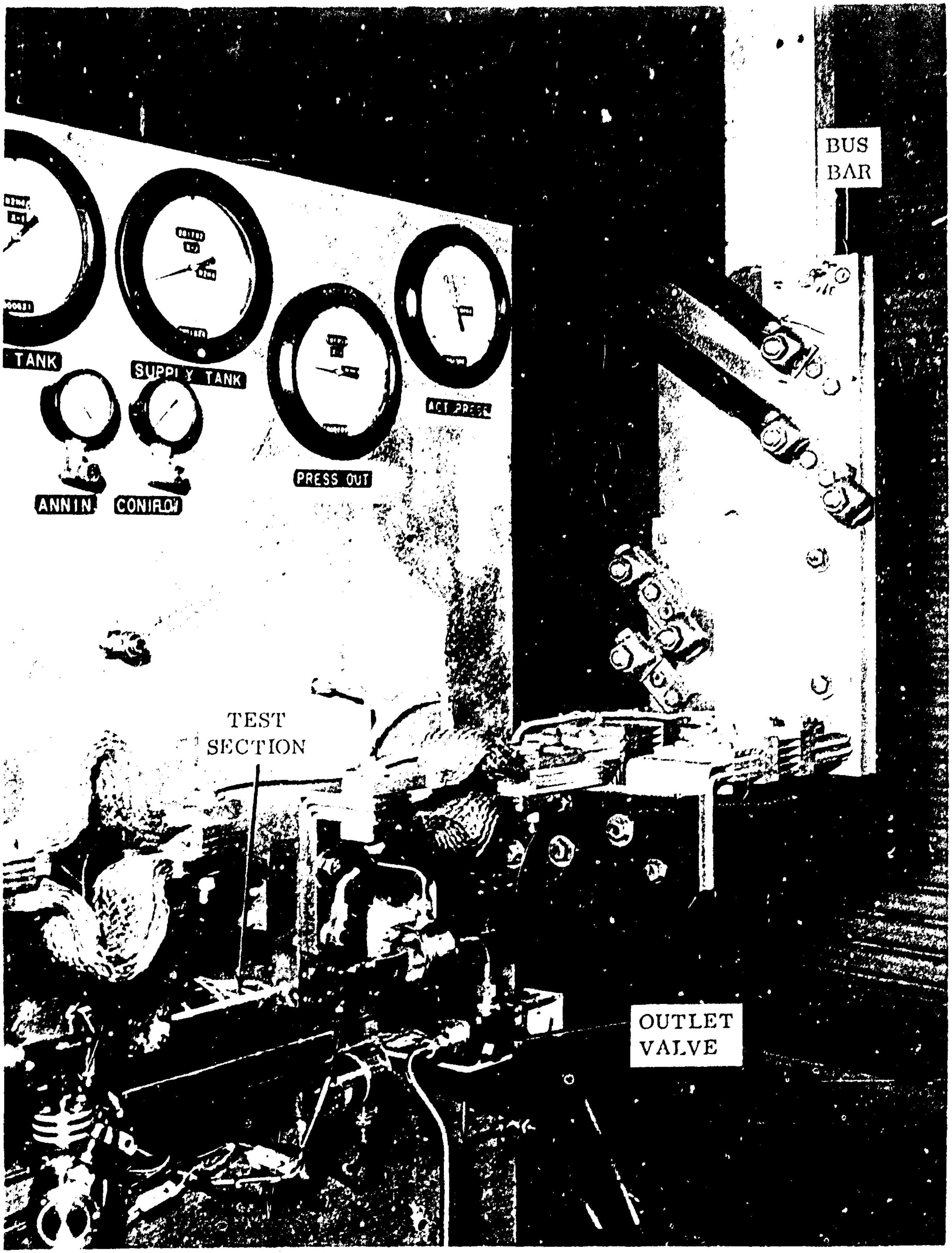

Figure 8. Test Apparatus - Right Side View

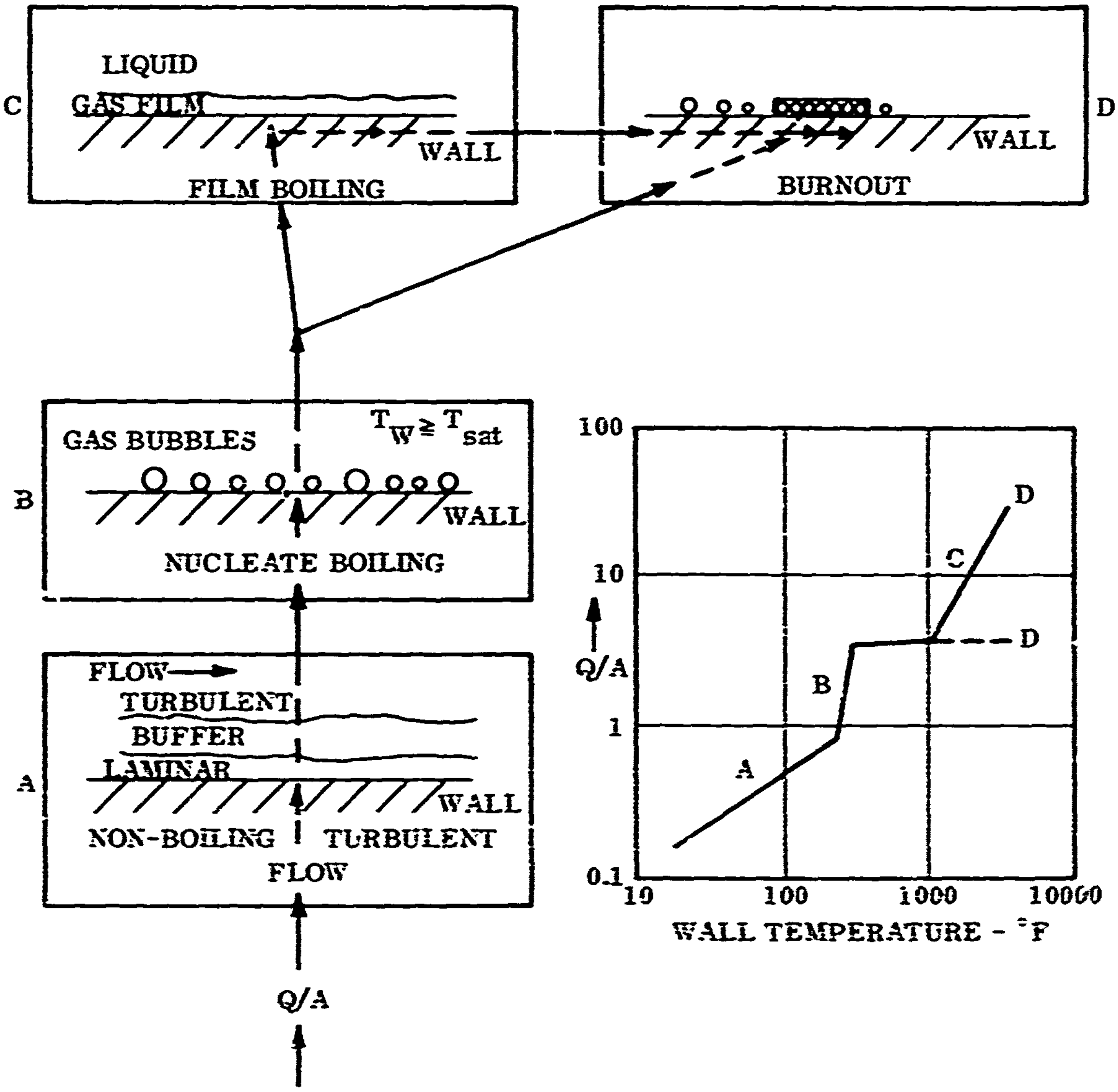

Figure 9. Forced Convection Heat Transfer Process

TEST NO: 1199 CELL: X-1
TEST DATE: 9-8-72
PROPELLANT TEMPERATURE: 32°F
INLET VELOCITY: 75 FPS
METAL TYPE: ALUMINUM
TUBE SIZE: 1/8 INCH
PROPELLANT TYPE: STANDARD HDA
TEST TYPE: W/O SHUTDOWN
PERCENT IMPURITY: 30 PPM IRON

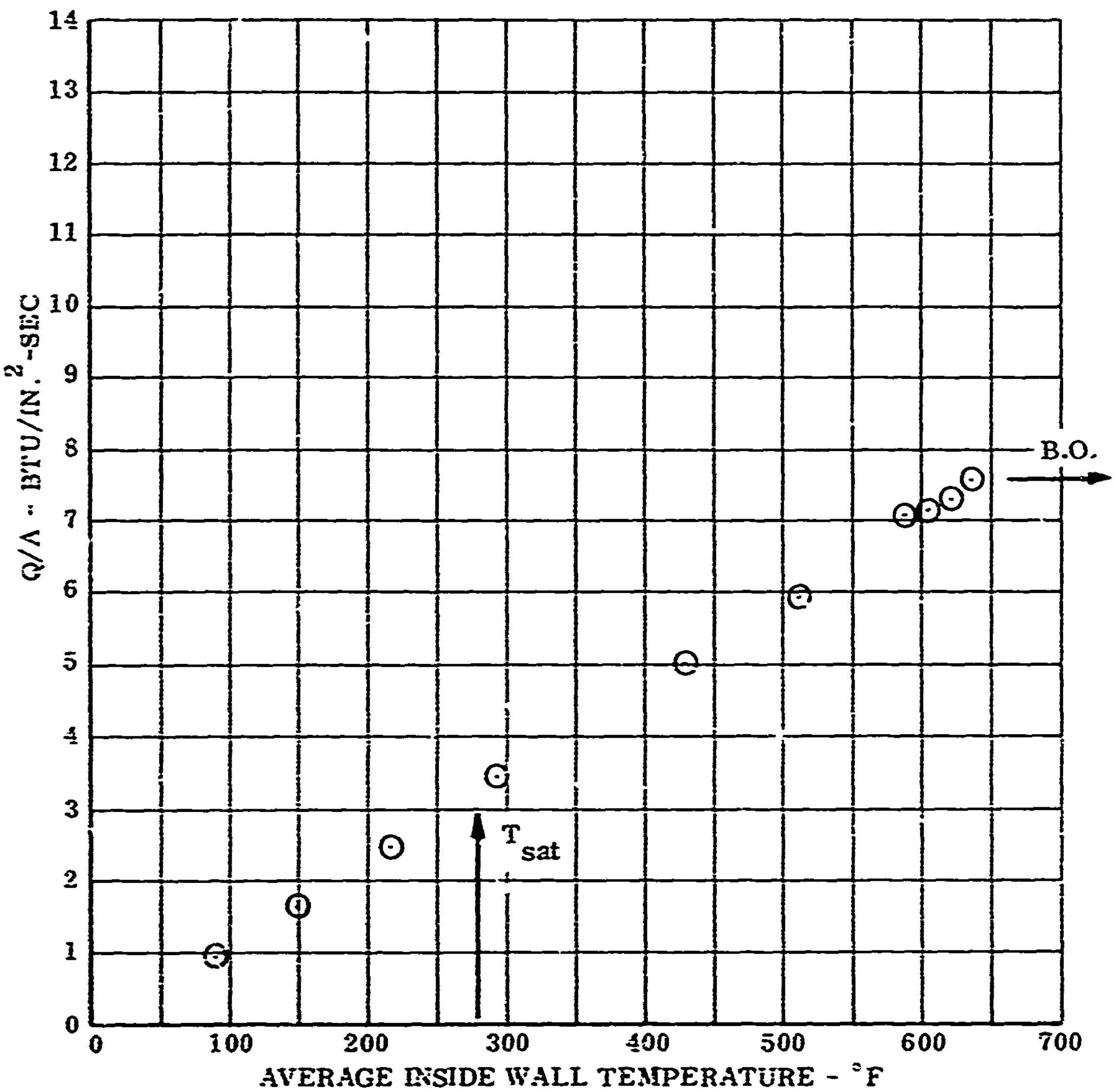

Figure 10. Heat Flux Versus Wall Temperature - Test 1199

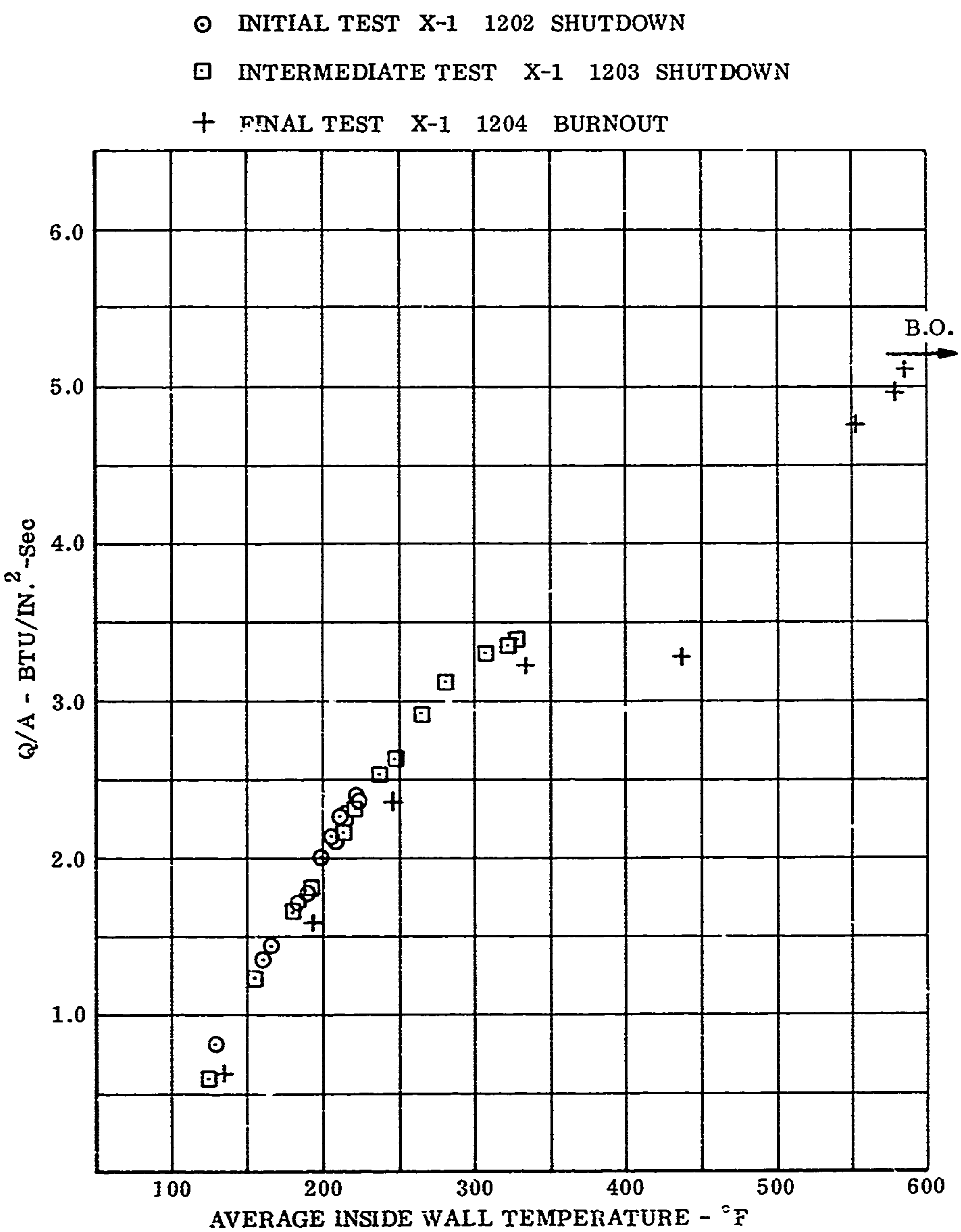

Figure 11. Effect Of Shutdown On Heat Transfer With Standard HDA Containing 30 PPM Iron Contaminant

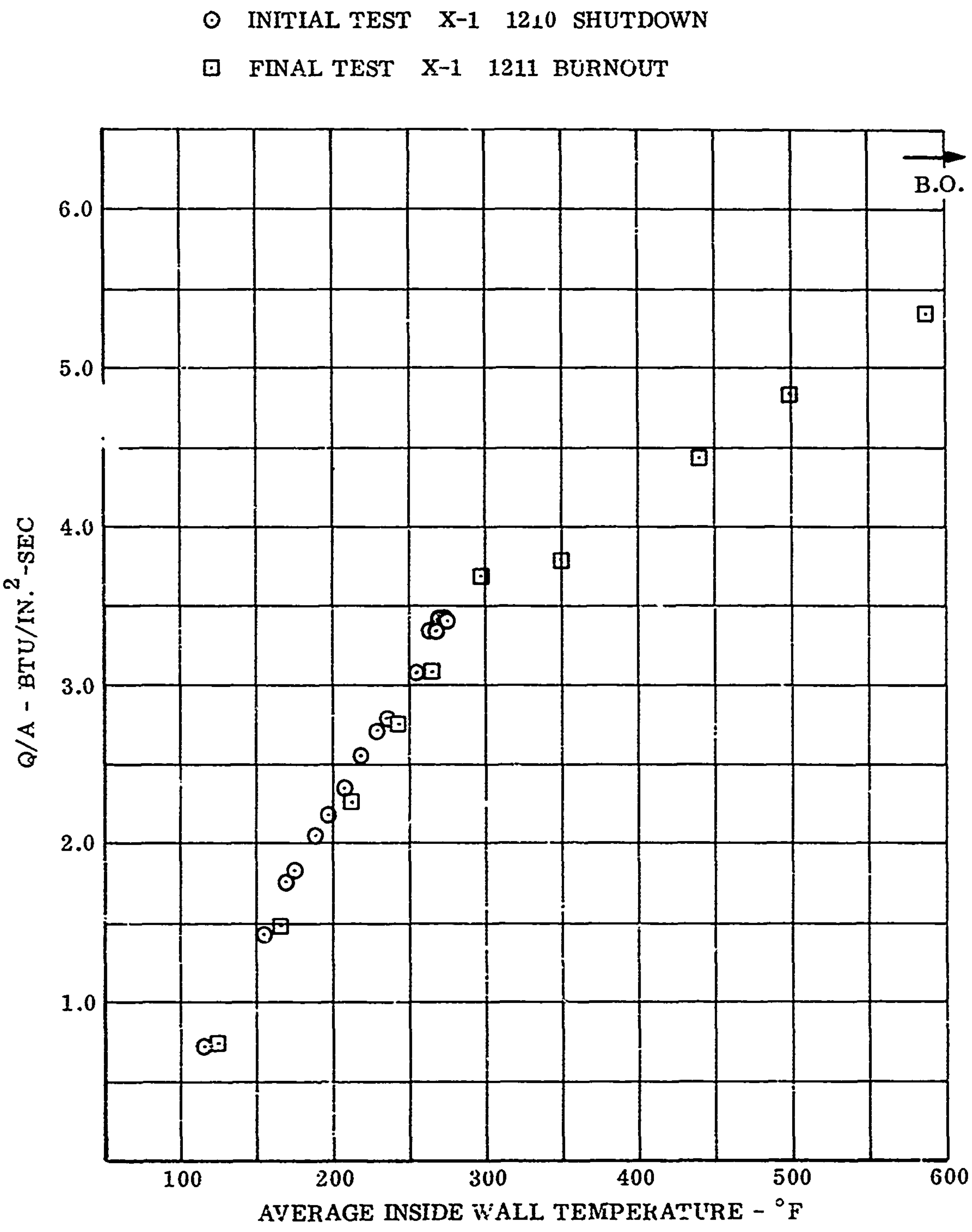

Figure 12. Effect Of Shutdown On Heat Transfer With Standard HDA Containing 55 PPM Iron Contaminant

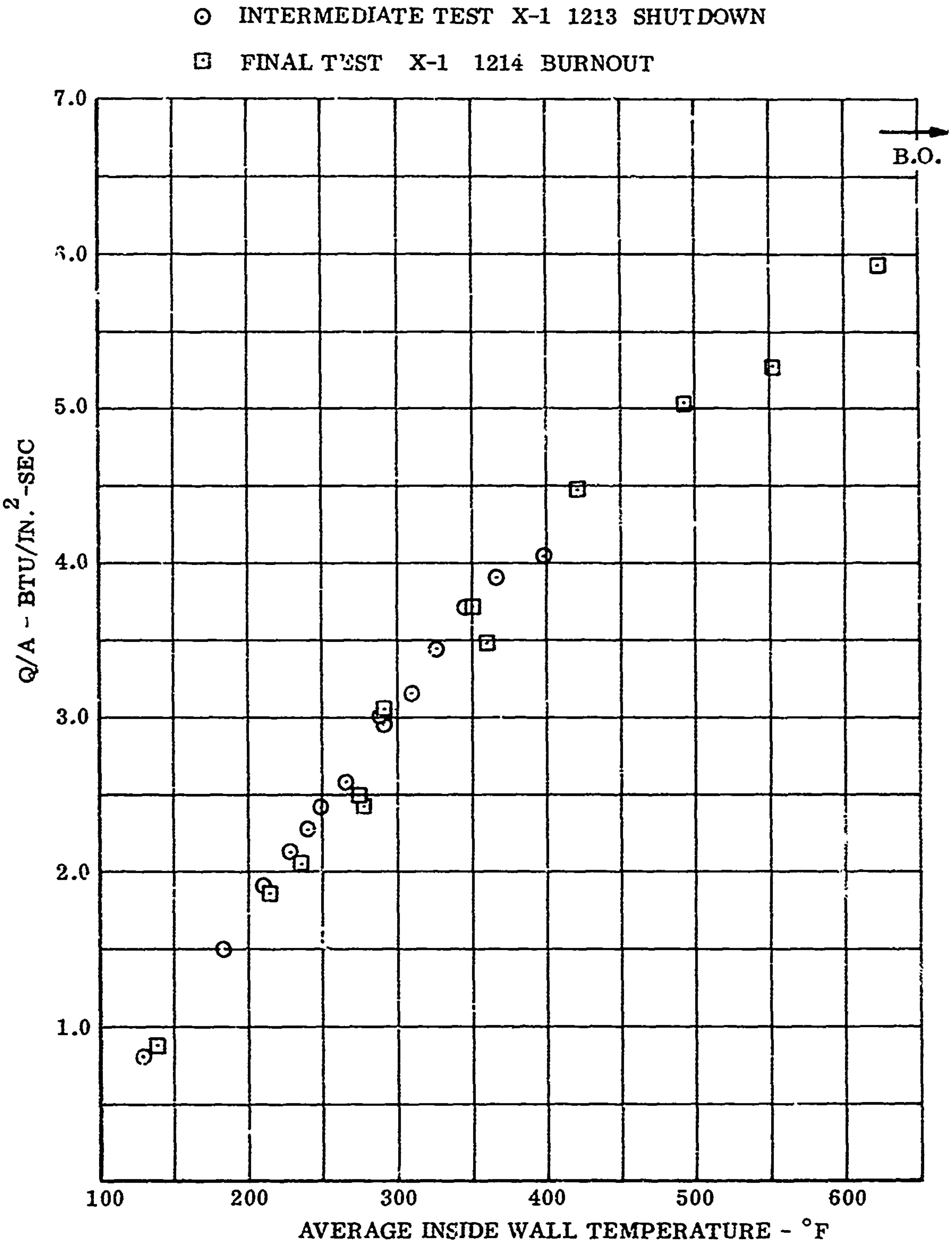

Figure 13. Effect Of Shutdown On Heat Transfer With Standard RDA Containing 72 PPM Iron Contaminant

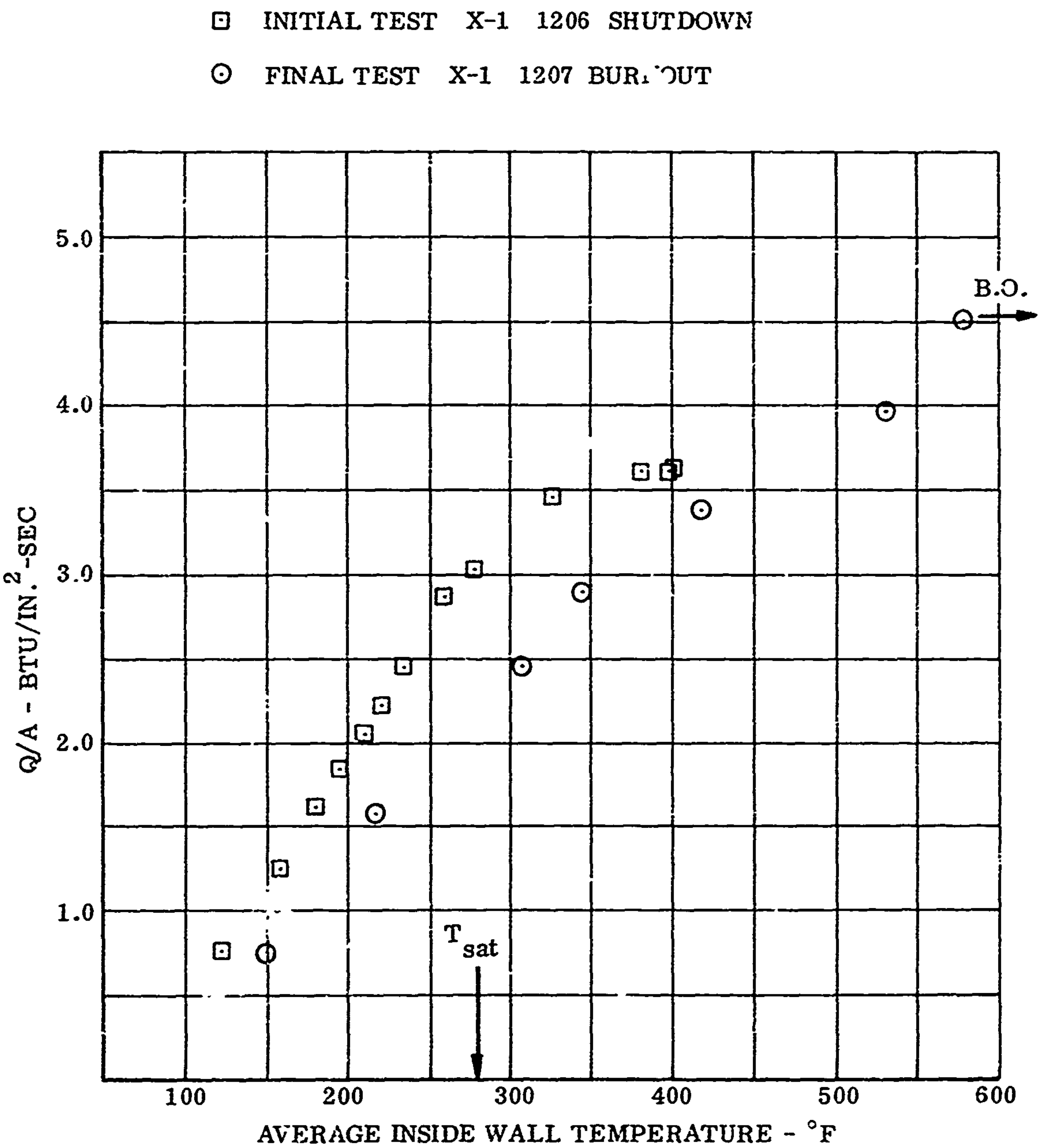

Figure 14. Effect Of Shutdown On Heat Transfer With Standard HDA Containing 96 PPM Iron Contaminant

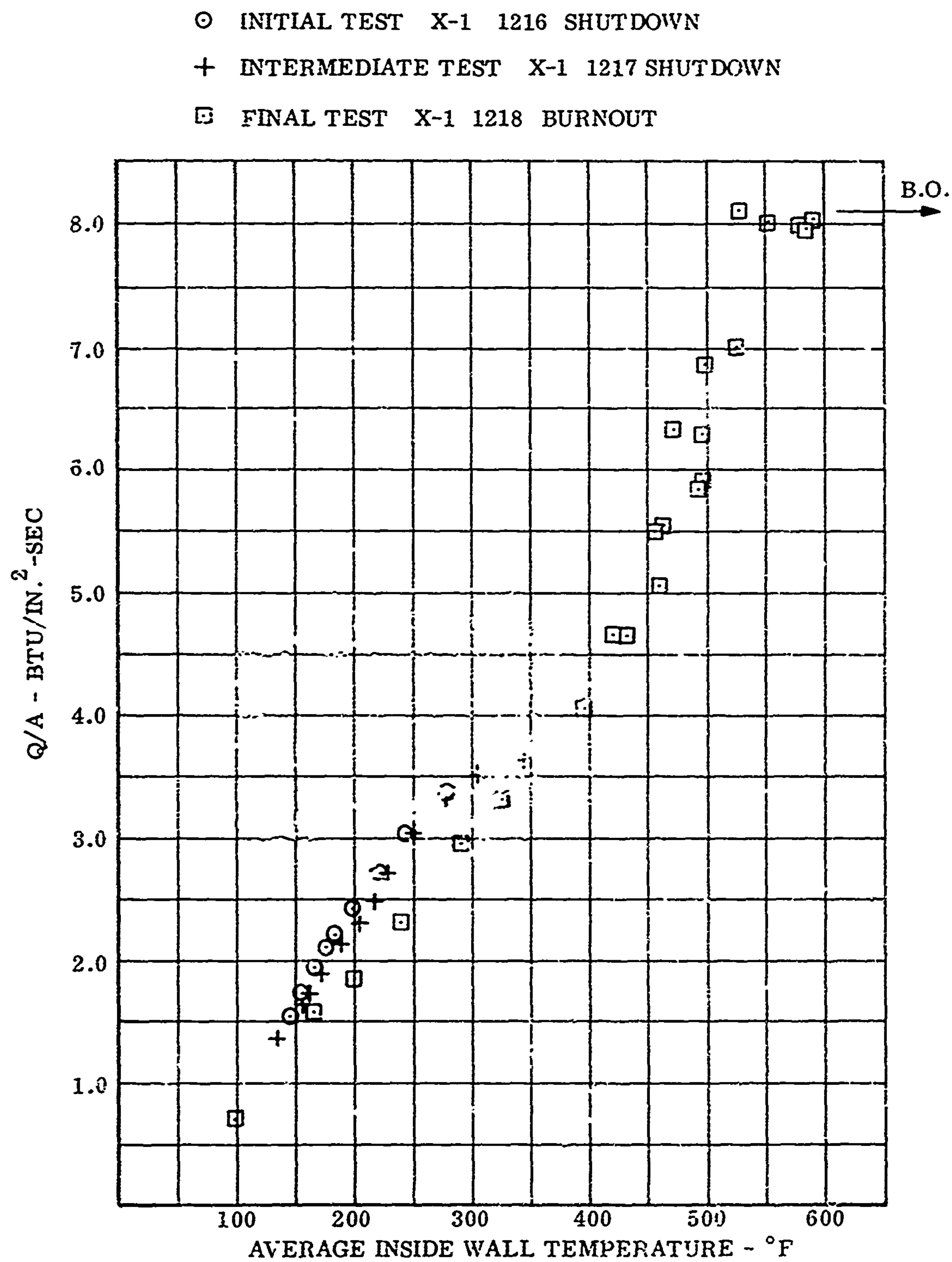

Figure 15. Effect Of Shutdown On Heat Transfer With Modified HDA (0.55% PF_5) Containing 10 PPM Iron Contaminant

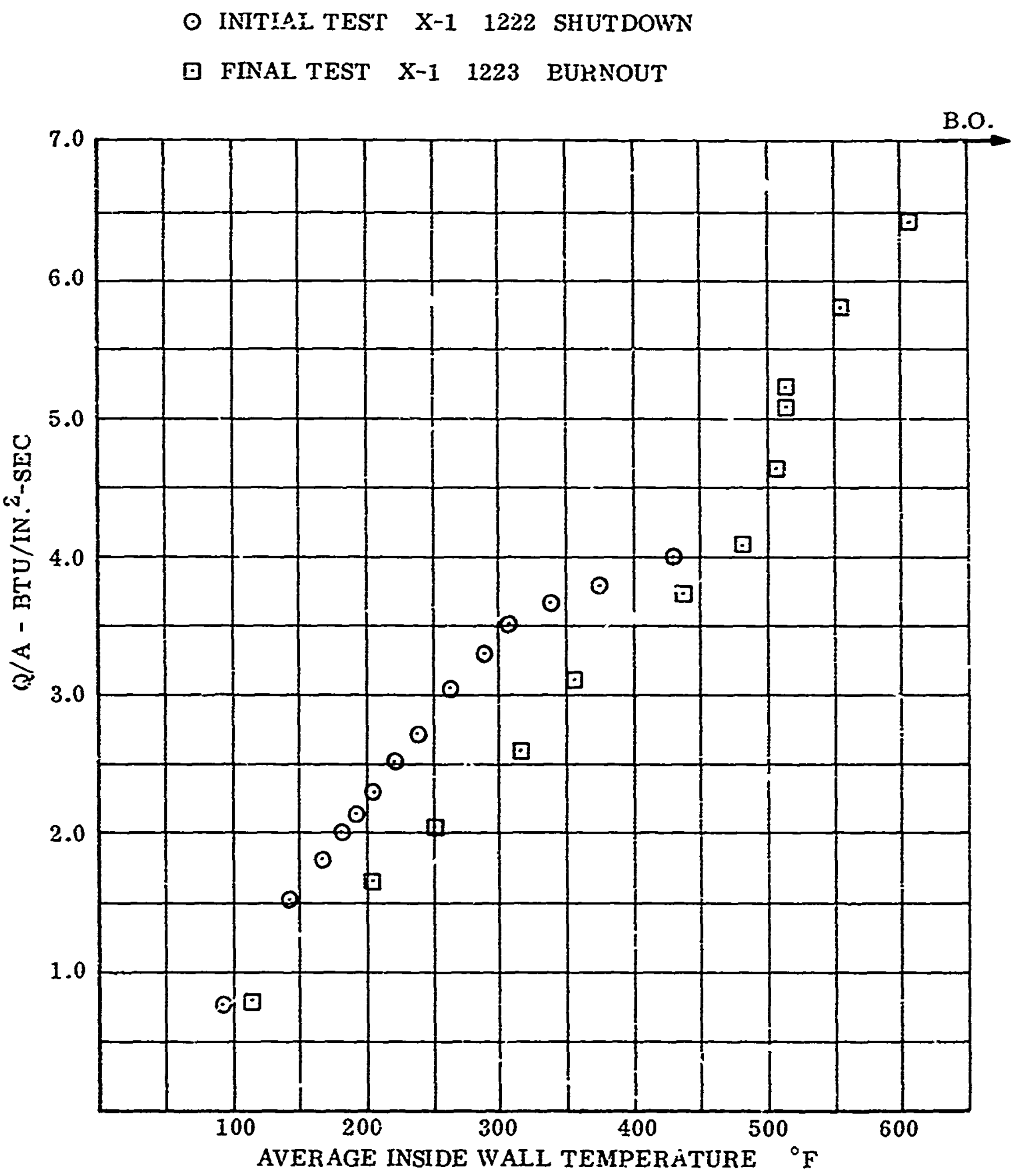

Figure 16. Effect Of Shutdown On Heat Transfer With Modified HDA (0.55% PF_5) Containing 50 PPM Iron Contaminant

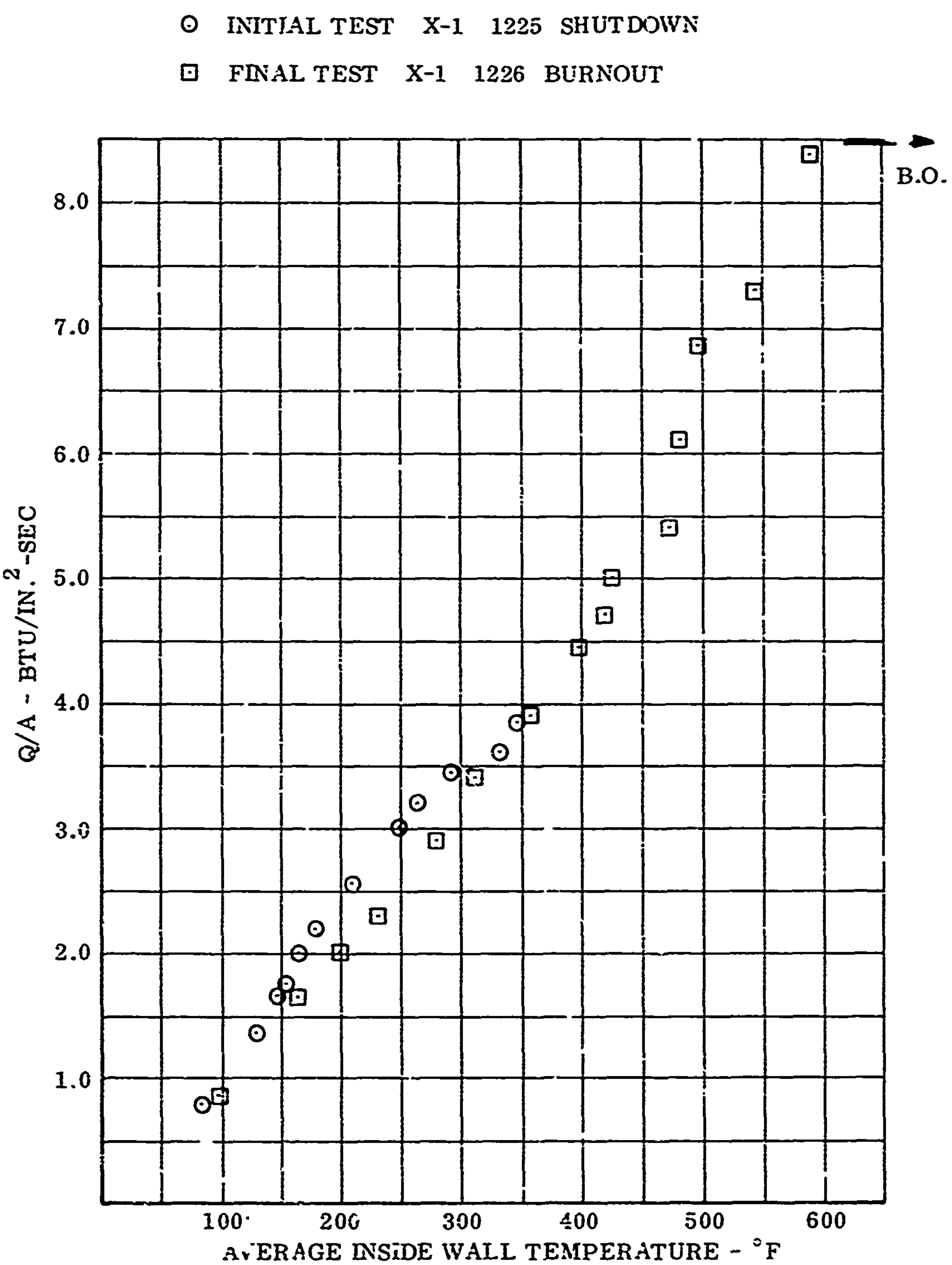

Figure 17. Effect Of Shutdown On Heat Transfer With Modified HDA (0.55% PF_5) Containing 97 PPM Iron Contaminant

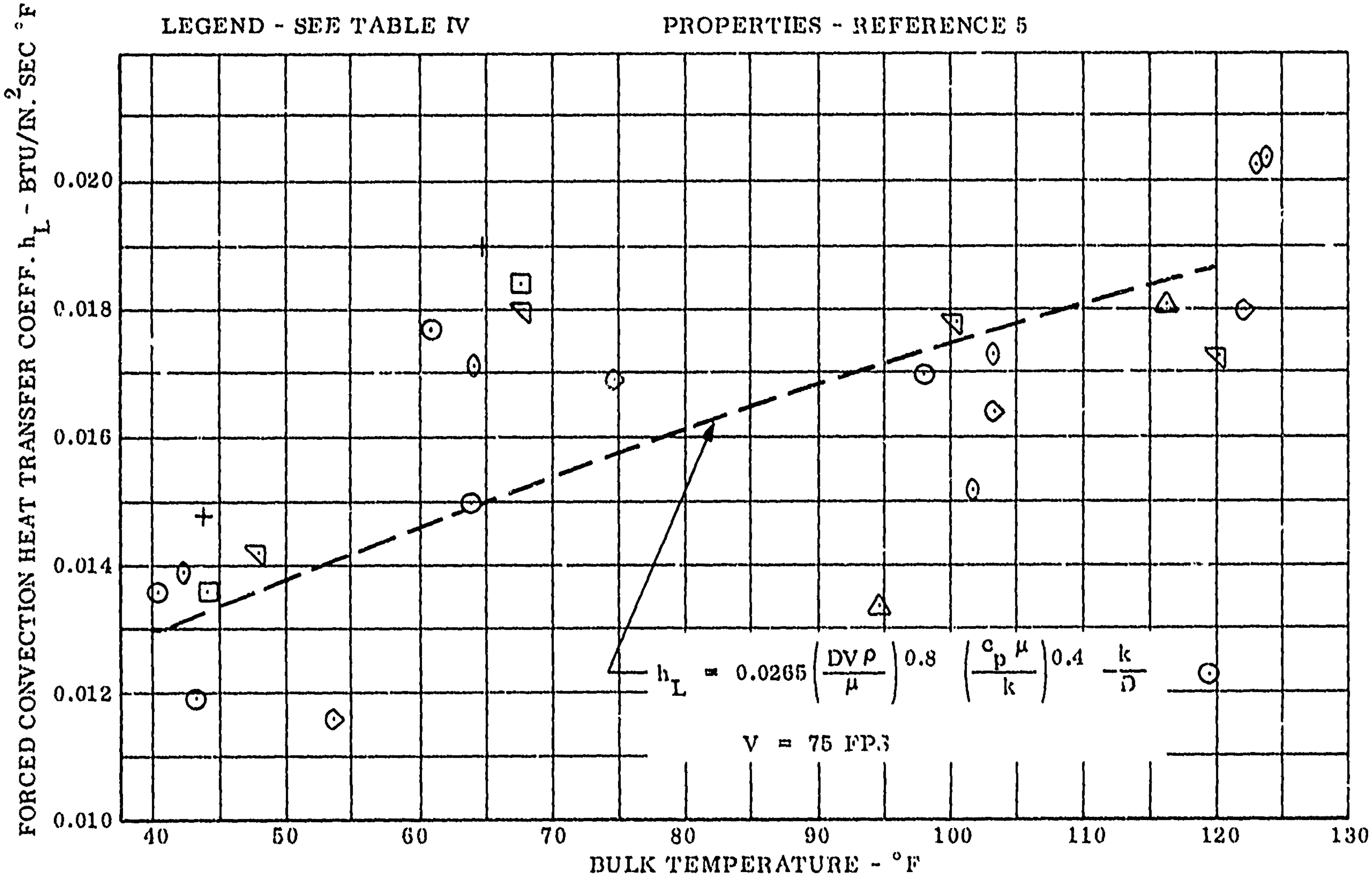

Figure 18. Effect Of Temperature On Heat Transfer Coefficient

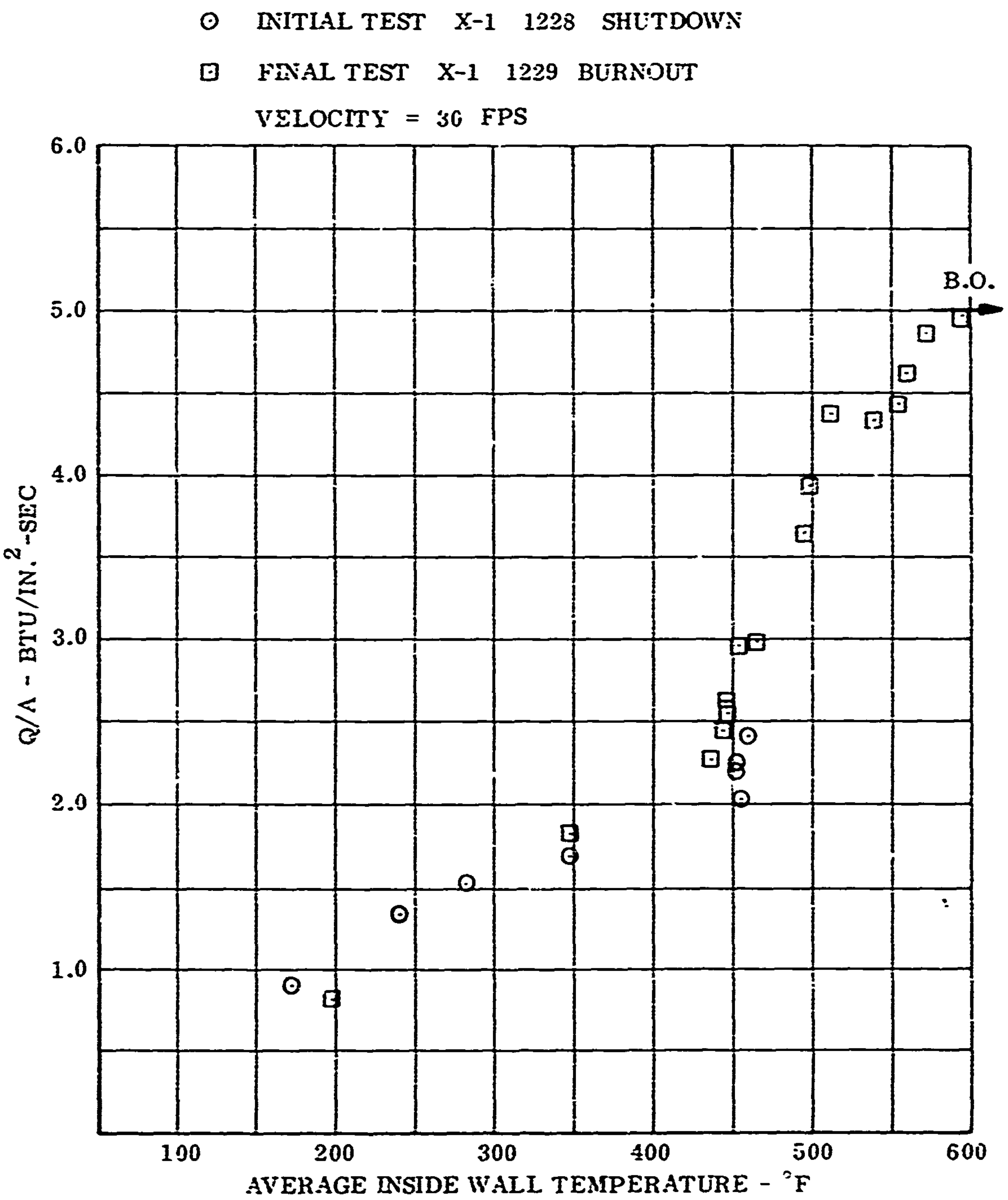

Figure 19. Effect Of Shutdown On Heat Transfer With Modified HDA (0.55% PF_5) Containing 92 PPM Iron Contaminant

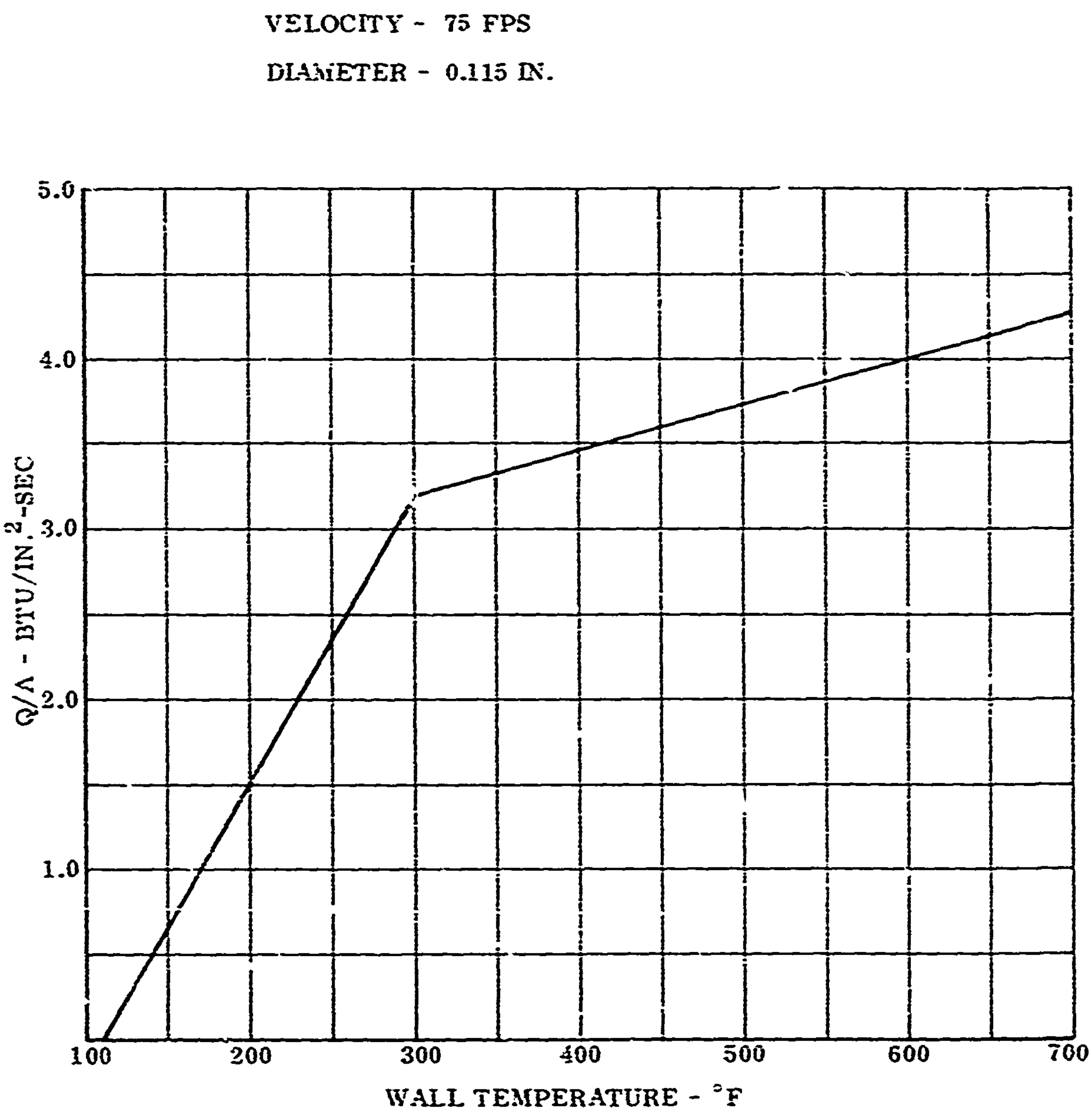

Figure 20. HDA Composite Coolant Characteristic

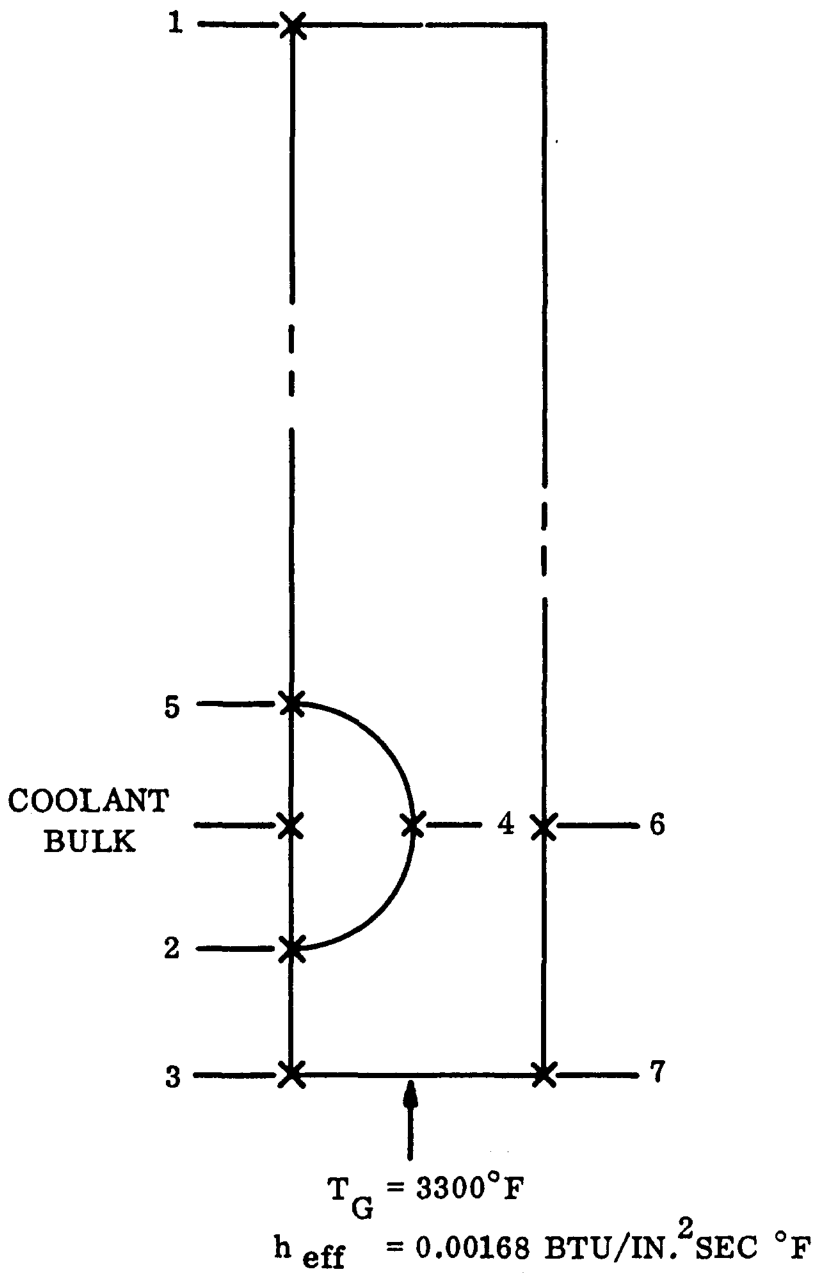

NODE	TEMPERATURE - °F	NODE	TEMPERATURE °F
1	180	4	229
2	373	5	169
3	501	6	238
COOLANT BULK	114	7	488

Figure 21. Agena Thrust Chamber Wall Element At Throat Station

TABLE I

HDA COMPOSITION (WEIGHT %)

	Standard	Modified
HNO_3	BAL	BAL
NO_2	42–46	42–46
H_2O	0.5 max.	0.5 max.
HF	0.6–0.8	- - -
PF_5	- - -	0.4–0.7
Total Nitrates	0.05 max.	0.05 max.
Fe_2O_3	0.003 max.	0.003 max.

TABLE II

TEST MATRIX

Test Number	Impurity PPM	Bulk Temperature - °F	HDA Type	Test Type
1	20	32	STD	W/O Shutdown
2	20	90		W/Shutdown
3	20	90		W/O Shutdown
4	60	32		W/O Shutdown
5	60	90		W/Shutdown
6	60	90		W/O Shutdown
7	100	32		W/O Shutdown
8	100	90		W/Shutdown
9	100	90	STD	W/O Shutdown
10	20	32	MOD	W/Shutdown
11	20	32		W/O Shutdown
12	20	90		W/O Shutdown
13	60	32		W/Shutdown
14	60	32		W/O Shutdown
15	60	90		W/O Shutdown
16	100	32		W/Shutdown
17	100	32		W/O Shutdown
18	100	90	MOD	W/O Shutdown
19 through 30 (1)				

The following conditions are fixed for all tests:

Velocity = 75 Fps

Bulk Pressure = 750 Psia

Tube Material -- 6061 Aluminum

Note (1): To be determined

TABLE III (1 of 9)

MEASURED AND DERIVED DATA - TEST 1199

	PARAMETER	UNITS									
TIME		SEC	4.0	5.0	6.0	4.0	5.0	6.0	4.0	5.0	6.0
1. VI	INLET FLOW VELOCITY	FPS	75.6	75.7	75.8	78.1	78.1	78.2	80.6	80.2	80.2
2. WP1	PROPELLANT FLOW NO.1	LBS/SEC	0.320	0.320	0.320	0.330	0.330	0.331	0.342	0.339	0.339
3. WP2	PROPELLANT FLOW NO.2	LBS/SEC	0.317	0.317	0.318	0.328	0.328	0.328	0.336	0.336	0.336
4. WPA	PROPELLANT FLOW AVG.	LBS/SEC	0.318	0.319	0.319	0.329	0.329	0.329	0.339	0.337	0.337
5. TL1	PROP.BULK TEMP.NO.1 IN LINE NEAR WP	DEG F	34.8	34.8	34.8	34.6	34.6	34.6	34.5	34.5	34.5
6. TL2	PROP.BULK TEMP.NO.2 IN LINE NEAR WP	DEG F	35.2	35.2	35.2	34.8	34.8	34.8	34.7	34.8	34.7
7. TLA	PROP.BULK TEMP.AVG. IN LINE NEAR WP	DEG F	35.0	35.0	35.0	34.7	34.7	34.7	34.6	34.6	34.6
8. SGC	SPECIFIC GRAVITY CORR TO TL ITEM 7		1.671	1.671	1.671	1.671	1.671	1.671	1.671	1.671	1.671
9. PI	FUEL PRESSURE AT TEST SECTION INLET	PSIA	864.4	864.2	864.1	859.7	859.7	859.6	854.5	854.5	854.4
10. PO	FUEL PRESSURE AT TEST SECTION OUTLET	PSIA	663.2	664.3	664.6	662.1	662.4	662.5	662.0	661.9	661.6
11. DELTA	CALCULATED PI-PO	PSID	201.2	199.9	199.5	197.6	197.3	197.1	192.5	192.7	192.8
12. DELTA	MEASURED DELTA	PSID	202.9	201.6	201.3	199.3	199.0	198.8	194.3	194.4	194.5
13. PT	TOTAL PRESSURE IN SUPPLY TANK	PSIA	951.2	951.3	951.3	952.2	952.2	952.3	951.7	951.7	951.7
14. PR	TOTAL PRESSURE IN RECEIVER TANK	PSIA	23.2	23.2	23.7	23.1	23.1	23.0	23.0	23.0	23.0
15. I1	AMPS PICKUP NO.1(AMPS FLOW BETWEEN ELEC.	AMPS	0.0	0.0	0.0	294.3	294.0	294.5	518.1	519.5	519.8
16. I2	AMPS PICKUP NO.2(AMPS FLOW BETWEEN ELEC.	AMPS	743.7	793.1	804.1	762.8	771.1	777.0	731.6	779.0	776.6
. IT	AMPS PICKUP TOT.(AMPS FLOW BETWEEN ELEC.	AMPS	743.7	793.1	804.1	1057.1	1065.1	1071.5	1299.7	1298.5	1296.4
18. DEL E	VOLTAGE DROP BETWEEN ELECTRODES	VOLTS	1.9	2.1	2.1	2.6	2.6	2.7	3.3	3.2	3.2
19. TI	PROP.BULK TEMP.AT TEST SECTION INLET	DEG F	35.8	35.8	35.8	35.4	35.4	35.4	35.1	35.2	35.2
22. TO	PROP.BULK TEMP.AT TEST SECTION OUTLET	DEG F	43.7	44.0	44.8	50.9	51.1	51.3	59.0	59.0	59.0
23. TS1	TEMP.OF TEST SECTIONS OUTER WALL STA-1	DEG F	92.5	94.4	98.2	157.9	158.8	160.1	233.9	233.4	233.0
24. TW1	TEMP.OF TEST SECTIONS INNER WALL STA-1	DEG F	89.0	90.4	94.2	151.3	152.1	153.3	224.0	223.5	223.1
25. TS2	TEMP.OF TEST SECTIONS OUTER WALL STA-2	DEG F	92.0	93.7	97.1	154.5	155.5	155.6	226.1	225.9	225.5
26. TW2	TEMP.OF TEST SECTIONS INNER WALL STA-2	DEG F	88.6	89.7	93.0	149.0	148.8	149.9	216.1	216.0	215.7
27. TS3	TEMP.OF TEST SECTIONS OUTER WALL STA-3	DEG F	92.7	94.5	98.0	157.1	158.0	159.2	229.0	229.1	228.6
28. TW3	TEMP.OF TEST SECTIONS INNER WALL STA-3	DEG F	89.3	90.5	93.9	150.5	151.4	152.4	219.1	219.2	218.8
29. TS4	TEMP.OF TEST SECTIONS OUTER WALL STA-4	DEG F	91.6	93.5	97.0	154.9	155.8	157.1	224.9	225.2	224.9
30. TW4	TEMP.OF TEST SECTIONS INNER WALL STA-4	DEG F	88.2	89.5	93.0	148.3	149.1	150.3	215.0	215.3	215.0
31. TS5	TEMP.OF TEST SECTIONS OUTER WALL STA-5	DEG F	94.8	96.9	100.5	158.9	159.9	161.1	229.8	229.9	229.8
32. TW5	TEMP.OF TEST SECTIONS INNER WALL STA-5	DEG F	91.3	92.9	96.4	152.4	153.2	154.3	219.9	220.0	219.9
	AVERAGE OF 5 STATIONS-OUTER WALL	DEG.F	92.7	94.6	98.2	156.7	157.6	158.6	228.6	228.7	228.4
	AVERAGE OF 5 STATIONS-INNER WALL	DEG.F	89.3	90.6	94.1	150.1	150.9	152.1	218.8	218.8	218.5
33. QIN	ENERGY TRANSFER INTO SYSTEM	BTU/SEC	1.4	1.6	1.6	2.6	2.7	2.7	4.0	4.0	4.0
34. QOUT	ENERGY TRANSFER OUT OF TEST AREA	BTU/SEC	1.1	1.1	1.2	2.2	2.2	2.2	3.5	3.4	3.4
35. ERROR	ENERGY BALANCE	PERCENT	22.23	29.24	24.70	17.09	17.30	17.21	13.62	14.01	13.58

TABLE III (2 of 9)

MEASURED AND DERIVED DATA - TEST 1199

	TIME	PARAMETER		UNITS SEC	4.0	5.0	6.0	4.0	5.0	6.0	4.0	5.0	6.0
45.	TB-1	LIQUID BULK TEMP. AT	STA-1	DEG F	37.8	37.8	34.	39.3	39.3	39.4	41.1	41.1	41.1
46.	TB-2	LIQUID BULK TEMP. AT	STA-2	DEG F	39.7	39.9	[illegible]	43.1	43.3	43.4	47.1	47.1	47.1
47.	TB-3	LIQUID BULK TEMP. AT	STA-3	DEG F	40.7	40.9	41.4	45.1	45.2	45.4	50.1	50.1	50.1
48.	TB-4	LIQUID BULK TEMP. AT	STA-4	DEG F	41.7	42.0	42.5	47.0	47.2	47.3	53.1	53.1	53.1
49.	TB-5	LIQUID BULK TEMP. AT	STA-5	DEG F	42.7	43.0	43.6	49.0	49.2	49.3	56.0	56.1	56.0
50.	S1-TB1	SATURATION TEMP.-BULK TEMP.	STA-1	DEG F	249.0	249.0	248.3	247.3	247.2	247.2	245.1	245.1	245.1
51.	S2-TB2	SATURATION TEMP.-BULK TEMP.	STA-2	DEG F	244.7	244.6	244.2	241.1	240.9	240.8	236.9	236.9	236.8
52.	S3-TB3	SATURATION TEMP.-BULK TEMP.	STA-3	DEG F	242.5	242.3	241.9	237.9	237.8	237.7	232.7	232.7	232.7
53.	S4-TB4	SATURATION TEMP.-BULK TEMP.	STA-4	DEG F	240.3	240.1	239.6	234.6	234.6	234.5	223.5	228.5	228.5
54.	S5-TB5	SATURATION TEMP.-BULK TEMP.	STA-5	DEG F	238.1	237.8	237.2	231.6	231.4	231.2	224.3	224.3	224.3
55.	PHI	HEAT FLUX-ALL STATIONS		BTU/SEC-IN2	0.846	0.975	1.000	1.620	1.649	1.670	2.473	2.467	2.455
56.	H-1	HEAT TRANSFER COEFFICIENT	STA-1	BTU/SEC-IN2-F	0.0165	0.0185	0.0178	0.0145	0.0146	0.0147	0.0135	0.0135	0.0135
57.	H-2	HEAT TRANSFER COEFFICIENT	STA-2	BTU/SEC-IN2-F	0.0173	0.0196	0.0190	0.0155	0.0156	0.0157	0.0146	0.0146	0.0146
58.	H-3	HEAT TRANSFER COEFFICIENT	STA-3	BTU/SEC-IN2-F	0.0174	0.0197	0.0190	0.0154	0.0155	0.0156	0.0146	0.0146	0.0146
59.	H-4	HEAT TRANSFER COEFFICIENT	STA-4	BTU/SEC-IN2-F	0.0182	0.0205	0.0198	0.0160	0.0162	0.0162	0.0153	0.0152	0.0152
60.	H-5	HEAT TRANSFER COEFFICIENT	STA-5	BTU/SEC-IN2-F	0.0174	0.0195	0.0189	0.0157	0.0158	0.0159	0.0151	0.0150	0.0153
61.	P-1	LIQUID STATIC PRESSURE	STA-1	PSIA	791.4	791.6	791.7	787.9	788.1	788.0	784.6	784.6	784.5
62.	P-2	LIQUID STATIC PRESSURE	STA-2	PSIA	763.8	764.2	764.4	760.9	761.0	761.0	758.2	758.2	758.0
63.	P-3	LIQUID STATIC PRESSURE	STA-3	PSIA	750.0	750.5	750.7	747.3	747.5	747.5	745.1	745.0	744.8
64.	P-4	LIQUID STATIC PRESSURE	STA-4	PSIA	736.2	736.3	737.0	733.8	734.0	734.0	731.9	731.8	731.6
65.	P-5	LIQUID STATIC PRESSURE	STA-5	PSIA	722.5	723.1	723.4	720.3	720.5	720.5	718.7	718.6	718.4
66.	REB	REYNOLDS NUMBER BULK			20071.	20120.	20194.	21274.	21301.	21339.	22512.	22496.	22497.
67.	REF-1	REYNOLDS NUMBER FILM	STA 1		23946.	24104.	24470.	30976.	31079.	31235.	40795.	40521.	40477.
68.	REF-2	REYNOLDS NUMBER FILM	STA 2		24078.	24218.	24566.	31039.	31140.	31299.	40553.	40323.	40289.
69.	REF-3	REYNOLDS NUMBER FILM	STA 3		24225.	24330.	24746.	31510.	31625.	31788.	41318.	41117.	41066.
70.	REF-4	REYNOLDS NUMBER FILM	STA 4		24215.	24387.	24762.	31479.	31597.	31773.	41179.	40996.	40966.
71.	REF-5	REYNOLDS NUMBER FILM	STA 5		24579.	24779.	25176.	32123.	32248.	32425.	42205.	41999.	41990.
72.	PRB	PRANDTL NUMBER BULK			24.857	24.871	24.809	24.333	24.315	24.297	23.701	23.698	23.698
73.	PRF-1	PRANDTL NUMBER FILM	STA 1		21.315	21.215	20.954	17.559	17.516	17.455	14.327	14.344	14.358
74.	PRF-2	PRANDTL NUMBER FILM	STA 2		21.212	21.128	20.883	17.534	17.487	17.426	14.397	14.402	14.412
75.	PRF-3	PRANDTL NUMBER FILM	STA 3		21.100	21.005	20.750	17.307	17.259	17.199	14.179	14.174	14.190
76.	PRF-4	PRANDTL NUMBER FILM	STA 4		21.108	21.000	20.739	17.321	17.272	17.255	14.218	14.208	14.218
77.	PRF-5	PRANDTL NUMBER FILM	STA 5		20.836	20.711	20.443	17.027	16.976	16.913	13.936	13.932	13.936

TABLE III (3 of 9)

MEASURED AND DERIVED DATA - TEST 1199

TIME	PARAMETER				UNITS SEC	4.0	5.0	6.0	4.0	5.0	6.0	4.0	5.0	5.0
78. NUB-1	NUSSELT	NUMBER	BULK	STA 1		353.1	396.4	381.1	310.0	313.3	314.4	290.7	290.8	290.0
79. NUB-2	NUSSELT	NUMBER	BULK	STA 2		370.5	418.9	405.7	331.5	335.0	336.2	314.5	314.0	313.0
80. NUB-3	NUSSELT	NUMBER	BULK	STA 3		372.8	420.7	407.5	329.5	333.1	334.4	314.5	313.6	312.8
81. NUB-4	NUSSELT	NUMBER	BULK	STA 4		389.5	438.2	424.1	343.0	346.8	347.8	328.3	326.9	325.9
82. NUB-5	NUSSELT	NUMBER	BULK	STA 5		372.3	417.6	405.2	336.1	339.8	341.1	324.4	323.4	322.0
83. NUF-1	NUSSELT	NUMBER	FILM	STA 1		358.2	402.3	387.2	320.6	324.1	325.5	308.5	306.5	307.5
84. NUF-2	NUSSELT	NUMBER	FILM	STA 2		376.1	425.3	412.3	342.9	346.6	348.0	333.5	333.0	331.9
85. NUF-3	NUSSELT	NUMBER	FILM	STA 3		378.5	427.4	414.3	341.4	345.2	346.7	334.3	333.3	332.5
86. NUF-4	NUSSELT	NUMBER	FILM	STA 4		395.5	445.2	431.3	355.4	359.4	360.5	348.8	347.4	346.2
87. NUF-5	NUSSELT	NUMBER	FILM	STA 5		378.5	424.8	412.7	348.9	352.9	354.4	345.8	344.7	343.2

TABLE III (4 of 9)

MEASURED AND DERIVED DATA - TEST 1199

	PARAMETER	UNITS									
TIME		SEC	4.0	5.0	6.0	4.0	5.0	6.0	16.0	29.0	30.0
1. VI	INLET FLOW VELOCITY	FPS	82.3	82.2	82.0	84.3	84.3	83.5	83.6	83.8	83.9
2. WP1	PROPELLANT FLOW NO.1	LBS/SEC	0.348	0.346	0.346	0.356	0.356	0.353	0.353	0.354	0.355
3. WP2	PROPELLANT FLOW NO.2	LBS/SEC	0.345	0.346	0.344	0.354	0.354	0.351	0.350	0.352	0.352
4. WPA	PROPELLANT FLOW AVG.	LBS/SEC	0.347	0.346	0.345	0.355	0.355	0.352	0.352	0.353	0.353
5. TL1	PROP.BULK TEMP.NO.1 IN LINE NEAR WP	DEG F	34.4	34.4	34.4	34.3	34.3	34.3	34.4	34.4	34.4
6. TL2	PROP.BULK TEMP.NO.2 IN LINE NEAR WP	DEG F	34.7	34.7	34.7	34.5	34.5	34.5	34.6	34.6	34.6
7. TLA	PROP.BULK TEMP.AVG. IN LINE NEAR WP	DEG F	34.6	34.5	34.5	34.4	34.4	34.4	34.5	34.5	34.5
8. SGC	SPECIFIC GRAVITY CORR TO TL ITEM 7		1.671	1.671	1.671	1.672	1.672	1.672	1.672	1.671	1.671
9. PI	FUEL PRESSURE AT TEST SECTION INLET	PSIA	849.6	850.6	850.7	846.4	846.4	848.3	849.2	849.6	849.6
10. PO	FUEL PRESSURE AT TEST SECTION OUTLET	PSIA	661.0	663.7	663.5	655.4	655.4	660.7	660.7	660.6	660.2
11. DELTA	CALCULATED PI-PO	PSID	188.6	187.0	187.2	191.0	191.0	187.6	188.5	189.0	189.3
12. DELTA	MEASURED DELTA	PSID	190.1	188.4	188.6	192.4	192.4	189.0	189.9	190.5	190.7
13. PT	TOTAL PRESSURE IN SUPPLY TANK	PSIA	951.7	951.7	951.7	952.9	952.9	952.9	953.8	954.3	954.4
14. PR	TOTAL PRESSURE IN RECEIVER TANK	PSIA	23.0	23.0	23.0	23.0	23.0	23.0	23.0	23.1	23.1
15. I1	AMPS PICKUP NO.1(AMPS FLOW BETWEEN ELEC.	AMPS	719.3	716.7	716.1	949.8	947.6	944.6	1035.5	1096.6	1093.5
16. I2	AMPS PICKUP NO.2(AMPS FLOW BETWEEN ELEC.	AMPS	780.0	777.1	776.8	770.1	769.4	769.3	769.6	764.3	772.1
17. IT	AMPS PICKUP TOT.(AMPS FLOW BETWEEN ELEC.	AMPS	1499.4	1493.8	1492.9	1719.9	1717.0	1714.0	1805.1	1860.9	1865.6
18. DEL E	VOLTAGE DROP BETWEEN ELECTRODES	VOLTS	4.0	3.9	3.9	5.0	5.0	5.0	5.7	6.5	6.5
19. TI	PROP.BULK TEMP.AT TEST SECTION INLET	DEG F	35.0	35.0	35.0	34.7	34.7	34.7	34.8	34.8	34.8
22. TO	PROP.BULK TEMP.AT TEST SECTION OUTLET	DEG F	68.2	68.0	68.0	82.8	82.8	82.9	92.3	101.7	102.3
23. TS1	TEMP.OF TEST SECTIONS OUTER WALL STA-1	DEG F	325.3	324.6	324.3	513.7	516.5	517.7	640.3	828.7	875.1
24. TW1	TEMP.OF TEST SECTIONS INNER WALL STA-1	DEG F	311.5	310.9	310.6	493.9	496.8	498.0	617.1	801.8	848.0
25. TS2	TEMP.OF TEST SECTIONS OUTER WALL STA-2	DEG F	306.7	305.7	305.3	459.6	463.8	466.2	597.9	692.9	706.5
26. TW2	TEMP.OF TEST SECTIONS INNER WALL STA-2	DEG F	292.9	292.0	291.6	439.8	444.0	446.4	574.7	665.7	679.0
27. TS3	TEMP.OF TEST SECTIONS OUTER WALL STA-3	DEG F	305.3	304.1	303.5	443.6	445.9	446.4	529.3	568.7	576.7
28. TW3	TEMP.OF TEST SECTIONS INNER WALL STA-3	DEG F	291.5	290.4	289.6	423.7	426.0	426.6	505.9	541.2	548.9
29. TS4	TEMP.OF TEST SECTIONS OUTER WALL STA-4	DEG F	299.7	298.4	297.8	427.7	429.5	429.8	489.2	540.4	551.2
30. TW4	TEMP.OF TEST SECTIONS INNER WALL STA-4	DEG F	285.9	284.7	284.1	407.7	409.7	410.0	465.8	512.8	523.4
31. TS5	TEMP.OF TEST SECTIONS OUTER WALL STA-5	DEG F	308.4	307.4	306.7	399.5	400.4	400.4	425.6	456.5	461.2
32. TW5	TEMP.OF TEST SECTIONS INNER WALL STA-5	DEG F	294.5	293.7	293.0	379.5	380.5	380.5	403.0	428.7	433.1
	AVERAGE OF 5 STATIONS-OUTER WALL	DEG.F	309.1	308.0	307.5	448.8	451.2	452.1	536.6	617.5	634.1
	AVERAGE OF 5 STATIONS-INNER WALL	DEG.F	295.2	294.3	293.8	428.9	431.4	432.3	513.3	590.0	606.5
33. QIN	ENERGY TRANSFER INTO SYSTEM	BTU/SEC	5.6	5.6	5.6	8.2	8.2	8.1	9.7	11.5	11.6
34. QOUT	ENERGY TRANSFER OUT OF TEST AREA	BTU/SEC	4.9	4.9	4.9	7.3	7.3	7.3	8.7	10.2	10.3
35. ERROR	ENERGY BALANCE	PERCENT	12.80	12.32	12.50	10.67	10.34	10.98	10.36	11.57	11.36

TABLE III (5 of 9)

MEASURED AND DERIVED DATA - TEST 1199

	PARAMETER			UNITS									
	TIME			SEC	4.0	5.0	6.0	4.0	5.0	6.0	16.0	29.0	30.0
45.	TB-1	LIQUID BULK TEMP. AT	STA-1	DEG F	43.3	43.2	43.2	46.7	46.7	46.7	49.2	51.5	51.6
46.	TB-2	LIQUID BULK TEMP. AT	STA-2	DEG F	51.6	51.5	51.5	58.8	58.8	58.8	63.6	68.2	68.5
47.	TB-3	LIQUID BULK TEMP. AT	STA-3	DEG F	55.7	55.6	55.6	64.8	64.8	64.8	70.8	76.6	77.0
48.	TB-4	LIQUID BULK TEMP. AT	STA-4	DEG F	59.9	59.7	59.7	70.8	70.8	70.8	78.0	85.0	85.4
49.	TB-5	LIQUID BULK TEMP. AT	STA-5	DEG F	64.0	63.9	63.8	76.8	76.8	76.8	85.2	93.4	93.9
50.	S1-TB1	SATURATION TEMP.-BULK TEMP.	STA-1	DEG F	242.6	242.8	242.9	238.8	238.8	239.1	236.7	234.4	234.3
51.	S2-TB2	SATURATION TEMP.-BULK TEMP.	STA-2	DEG F	232.1	232.4	232.4	224.5	224.5	224.8	220.1	215.4	215.1
52.	S3-TB3	SATURATION TEMP.-BULK TEMP.	STA-3	DEG F	226.8	227.1	227.1	217.4	217.3	217.7	211.8	205.9	205.5
53.	S4-TB4	SATURATION TEMP.-BULK TEMP.	STA-4	DEG F	221.5	221.8	221.9	210.2	210.1	210.5	203.4	196.4	195.9
54.	S5-TB5	SATURATION TEMP.-BULK TEMP.	STA-5	DEG F	216.2	216.5	216.6	202.9	202.9	203.3	195.0	186.8	186.3
55.	PHI	HEAT FLUX-ALL STATIONS		BTU/SEC-IN2	3.470	3.437	3.430	5.051	5.037	5.025	5.978	7.083	7.142
56.	H-1	HEAT TRANSFER COEFFICIENT	STA-1	BTU/SEC-IN2-F	0.0129	0.0128	0.0128	0.0113	0.0112	0.0111	0.0105	0.0094	0.0090
57.	H-2	HEAT TRANSFER COEFFICIENT	STA-2	BTU/SEC-IN2-F	0.0144	0.0143	0.0143	0.0133	0.0131	0.0130	0.0117	0.0119	0.0117
58.	H-3	HEAT TRANSFER COEFFICIENT	STA-3	BTU/SEC-IN2-F	0.0147	0.0146	0.0146	0.0141	0.0139	0.0139	0.0137	0.0152	0.0151
59.	H-4	HEAT TRANSFER COEFFICIENT	STA-4	BTU/SEC-IN2-F	0.0154	0.0153	0.0153	0.0150	0.0149	0.0148	0.0154	0.0166	0.0163
60.	H-5	HEAT TRANSFER COEFFICIENT	STA-5	BTU/SEC-IN2-F	0.0151	0.0150	0.0150	0.0167	0.0166	0.0165	0.0188	0.0211	0.0211
61.	P-1	LIQUID STATIC PRESSURE	STA-1	PSIA	781.2	782.8	782.7	777.0	777.1	780.2	780.8	781.0	780.8
62.	P-2	LIQUID STATIC PRESSURE	STA-2	PSIA	755.3	757.1	757.1	750.9	750.9	754.5	754.9	755.1	754.9
63.	P-3	LIQUID STATIC PRESSURE	STA-3	PSIA	742.4	744.3	744.2	737.8	737.8	741.7	742.0	742.1	741.9
64.	P-4	LIQUID STATIC PRESSURE	STA-4	PSIA	729.5	731.5	731.4	724.7	724.8	728.8	729.1	729.2	729.0
65.	P-5	LIQUID STATIC PRESSURE	STA-5	PSIA	716.6	718.7	718.6	711.6	711.7	716.0	716.2	716.2	716.0
66.	REB	REYNOLDS NUMBER BULK			23893.	23855.	23766.	25809.	25815.	25565.	26495.	27496.	27595.
67.	REF-1	REYNOLDS NUMBER FILM	STA 1		54455.	54314.	54077.	88513.	89061.	88433.	111675.	144377.	151003.
68.	REF-2	REYNOLDS NUMBER FILM	STA 2		52883.	52688.	52443.	80591.	81386.	81052.	106334.	124592.	127233.
69.	REF-3	REYNOLDS NUMBER FILM	STA 3		53294.	53066.	52797.	78729.	79180.	78516.	94554.	102748.	104471.
70.	REF-4	REYNOLDS NUMBER FILM	STA 4		53078.	52839.	52548.	76912.	77279.	76582.	88298.	98905.	101177.
71.	REF-5	REYNOLDS NUMBER FILM	STA 5		55029.	54836.	54530.	72903.	73083.	72385.	77972.	84496.	85544.
72.	PRB	PRANDTL NUMBER BULK			23.004	23.021	23.024	21.956	21.955	21.954	21.292	20.673	20.635
73.	PRF-1	PRANDTL NUMBER FILM	STA 1		11.588	11.604	11.612	8.394	8.363	8.350	7.403	7.113	7.251
74.	PRF-2	PRANDTL NUMBER FILM	STA 2		11.853	11.879	11.890	8.904	8.849	8.816	7.563	7.146	7.115
75.	PRF-3	PRANDTL NUMBER FILM	STA 3		11.782	11.814	11.828	9.042	9.009	9.001	8.035	7.701	7.644
76.	PRF-4	PRANDTL NUMBER FILM	STA 4		11.819	11.853	11.871	9.184	9.156	9.152	8.361	7.853	7.767
77.	PRF-5	PRANDTL NUMBER FILM	STA 5		11.496	11.520	11.538	9.526	9.510	9.509	9.047	8.607	8.549

TABLE III (6 of 9)

MEASURED AND DERIVED DATA - TEST 1199

TIME	PARAMETER				UNITS SEC	4.0	5.0	6.0	4.0	5.0	6.0	16.0	29.0	30.0
78. NUB-1	NUSSELT	NUMBER	BULK	STA 1		278.9	276.7	276.4	244.5	242.3	241.0	228.5	205.6	195.3
79. NUB-2	NUSSELT	NUMBER	BULK	STA 2		310.0	308.0	307.8	287.0	283.1	280.6	254.0	258.2	254.8
80. NUB-3	NUSSELT	NUMBER	BULK	STA 3		317.3	315.5	315.5	304.7	301.8	300.6	298.3	332.0	329.6
81. NUB-4	NUSSELT	NUMBER	BULK	STA 4		330.9	329.2	329.4	324.5	321.8	320.7	334.7	360.6	355.2
82. NUB-5	NUSSELT	NUMBER	BULK	STA 5		324.5	322.3	322.5	351.2	359.1	358.2	408.4	460.0	458.6
83. NUF-1	NUSSELT	NUMBER	FILM	STA 1		306.9	304.4	304.0	296.1	293.9	292.6	300.8	318.4	318.0
84. NUF-2	NUSSELT	NUMBER	FILM	STA 2		339.4	337.1	336.8	338.8	335.0	332.6	327.4	357.7	357.0
85. NUF-3	NUSSELT	NUMBER	FILM	STA 3		347.9	345.8	345.7	357.6	354.8	353.5	368.5	420.6	419.8
86. NUF-4	NUSSELT	NUMBER	FILM	STA 4		362.6	360.5	360.7	378.8	376.0	374.8	404.9	453.5	447.0
87. NUF-5	NUSSELT	NUMBER	FILM	STA 5		357.6	355.0	355.2	416.4	414.2	413.2	477.9	547.5	547.3

TABLE III (7 of 9)

MEASURED AND DERIVED DATA - TEST 1199

	PARAMETER	UNITS		
TIME		SEC	31.0	32.0
1. VI	INLET FLOW VELOCITY	FPS	84.1	85.7
2. WP1	PROPELLANT FLOW NO.1	LBS/SEC	0.355	0.367
3. WP2	PROPELLANT FLOW NO.2	LBS/SEC	0.353	0.364
4. WPA	PROPELLANT FLOW AVG.	LBS/SEC	0.354	0.365
5. TL1	PROP.BULK TEMP.NO.1 IN LINE NEAR WP	DEG F	34.4	34.4
6. TL2	PROP.BULK TEMP.NO.2 IN LINE NEAR WP	DEG F	34.6	34.6
7. TLA	PROP.BULK TEMP.AVG. IN LINE NEAR WP	DEG F	34.5	34.5
8. SGC	SPECIFIC GRAVITY CORR TO TL ITEM 7		1.672	1.671
9. PI	FUEL PRESSURE AT TEST SECTION INLET	PSIA	849.3	842.6
10. PO	FUEL PRESSURE AT TEST SECTION OUTLET	PSIA	661.2	657.0
11. DELTA	CALCULATED PI-PO	PSID	188.1	185.6
12. DELTA	MEASURED DELTA	PSID	189.6	187.0
13. PT	TOTAL PRESSURE IN SUPPLY TANK	PSIA	954.3	954.4
14. PR	TOTAL PRESSURE IN RECEIVER TANK	PSIA	23.1	23.1
15. I1	AMPS PICKUP NO.1(AMPS FLOW BETWEEN ELEC.	AMPS	1103.8	1127.6
16. I2	AMPS PICKUP NO.2(AMPS FLOW BETWEEN ELEC.	AMPS	773.4	777.0
17. IT	AMPS PICKUP TOT.(AMPS FLOW BETWEEN ELEC.	AMPS	1877.1	1904.6
18. DEL E	VOLTAGE DROP BETWEEN ELECTRODES	VOLTS	6.7	6.8
19. TI	PROP.BULK TEMP.AT TEST SECTION INLET	DEG F	34.8	34.8
22. TO	PROP.BULK TEMP.AT TEST SECTION OUTLET	DEG F	103.0	104.8
23. TS1	TEMP.OF TEST SECTIONS OUTER WALL STA-1	DEG F	917.0	936.1
24. TW1	TEMP.OF TEST SECTIONS INNER WALL STA-1	DEG F	889.4	907.5
25. TS2	TEMP.OF TEST SECTIONS OUTER WALL STA-2	DEG F	716.6	732.0
26. TW2	TEMP.OF TEST SECTIONS INNER WALL STA-2	DEG F	688.5	703.0
27. TS3	TEMP.OF TEST SECTIONS OUTER WALL STA-3	DEG F	589.0	604.3
28. TW3	TEMP.OF TEST SECTIONS INNER WALL STA-3	DEG F	559.5	574.9
29. TS4	TEMP.OF TEST SECTIONS OUTER WALL STA-4	DEG F	563.8	582.1
30. TW4	TEMP.OF TEST SECTIONS INNER WALL STA-4	DEG F	535.3	552.6
31. TS5	TEMP.OF TEST SECTIONS OUTER WALL STA-5	DEG F	465.0	474.3
32. TW5	TEMP.OF TEST SECTIONS INNER WALL STA-5	DEG F	436.2	444.5
	AVERAGE OF 5 STATIONS-OUTER WALL	DEG.F	650.1	645.8
	AVERAGE OF 5 STATIONS-INNER WALL	DEG.F	621.8	636.5
33. QIN	ENERGY TRANSFER INTO SYSTEM	BTU/SEC	11.9	12.3
34. QOUT	ENERGY TRANSFER OUT OF TEST AREA	BTU/SEC	10.4	11.0
35. ERROR	ENERGY BALANCE	PERCENT	12.49	10.57

TABLE III (8 of 9)

MEASURED AND DERIVED DATA - TEST 1199

	PARAMETER		UNITS		
TIME			SEC	31.0	32.0
45. TB-1	LIQUID BULK TEMP. AT	STA-1	DEG F	51.8	52.3
46. TB-2	LIQUID BULK TEMP. AT	STA-2	DEG F	68.9	69.8
47. TB-3	LIQUID BULK TEMP. AT	STA-3	DEG F	77.4	78.6
48. TB-4	LIQUID BULK TEMP. AT	STA-4	DEG F	86.0	87.3
49. TB-5	LIQUID BULK TEMP. AT	STA-5	DEG F	94.5	96.1
50. S1-TB1	SATURATION TEMP.-BULK TEMP.	STA-1	DEG F	234.1	233.1
51. S2-TB2	SATURATION TEMP.-BULK TEMP.	STA-2	DEG F	214.8	213.4
52. S3-TB3	SATURATION TEMP.-BULK TEMP.	STA-3	DEG F	205.1	203.5
53. S4-TB4	SATURATION TEMP.-BULK TEMP.	STA-4	DEG F	195.4	193.6
54. S5-TB5	SATURATION TEMP.-BULK TEMP.	STA-5	DEG F	185.7	183.7
55. PHI	HEAT FLUX-ALL STATIONS		BTU/SEC-IN2	7.320	7.581
56. H-1	HEAT TRANSFER COEFFICIENT	STA-1	BTU/SEC-IN2-F	0.0087	0.0089
57. H-2	HEAT TRANSFER COEFFICIENT	STA-2	BTU/SEC-IN2-F	0.0118	0.0120
58. H-3	HEAT TRANSFER COEFFICIENT	STA-3	BTU/SEC-IN2-F	0.0152	0.0153
59. H-4	HEAT TRANSFER COEFFICIENT	STA-4	BTU/SEC-IN2-F	0.0163	0.0163
60. H-5	HEAT TRANSFER COEFFICIENT	STA-5	BTU/SEC-IN2-F	0.0214	0.0219
61. P-1	LIQUID STATIC PRESSURE	STA-1	PSIA	781.0	775.2
62. P-2	LIQUID STATIC PRESSURE	STA-2	PSIA	755.2	749.8
63. P-3	LIQUID STATIC PRESSURE	STA-3	PSIA	742.4	737.1
64. P-4	LIQUID STATIC PRESSURE	STA-4	PSIA	729.5	724.4
65. P-5	LIQUID STATIC PRESSURE	STA-5	PSIA	716.6	711.7
66. REB	REYNOLDS NUMBER BULK			27708.	28775.
67. REF-1	REYNOLDS NUMBER FILM	STA 1		156182.	163140.
68. REF-2	REYNOLDS NUMBER FILM	STA 2		129171.	136026.
69. REF-3	REYNOLDS NUMBER FILM	STA 3		106750.	113394.
70. REF-4	REYNOLDS NUMBER FILM	STA 4		103733.	110715.
71. REF-5	REYNOLDS NUMBER FILM	STA 5		86387.	91351.
72. PRB	PRANDTL NUMBER BULK			20.589	20.471
73. PRF-1	PRANDTL NUMBER FILM	STA 1		7.455	7.574
74. PRF-2	PRANDTL NUMBER FILM	STA 2		7.097	7.675
75. PRF-3	PRANDTL NUMBER FILM	STA 3		7.571	7.472
76. PRF-4	PRANDTL NUMBER FILM	STA 4		7.676	7.553
77. PRF-5	PRANDTL NUMBER FILM	STA 5		8.505	8.395

TABLE III (9 of 9)

MEASURED AND DERIVED DATA - TEST 1199

	PARAMETER				UNITS		
TIME					SEC	31.0	32.0
78. NUB-1	NUSSFLT	NUMBER	BULK	STA 1		190.4	193.2
79. NUB-2	NUSSELT	NUMBER	BULK	STA 2		257.4	261.0
80. NUB-3	NUSSELT	NUMBER	BULK	STA 3		330.8	333.0
81. NUB-4	NUSSELT	NUMBER	BULK	STA 4		354.9	355.2
82. NUB-5	NUSSELT	NUMBER	BULK	STA 5		466.7	474.2
83. NUF-1	NUSSELT	NUMBER	FILM	STA 1		325.3	337.6
84. NUF-2	NUSSELT	NUMBER	FILM	STA 2		363.7	373.7
85. NUF-3	NUSSELT	NUMBER	FILM	STA 3		424.6	432.3
86. NUF-4	NUSSELT	NUMBER	FILM	STA 4		450.4	456.6
87. NUF-5	NUSSELT	NUMBER	FILM	STA 5		558.1	570.3

TABLE IV (1 of 2)

SUMMARY OF HDA HEAT TRANSFER TESTS

Symbols (4)	Test Number		Iron Impurity Level PPM Fe_2O_3	Test Type (1)	Inlet Propellant Temperature °F		Inlet Velocity FPS	Bulk Propellant Temperature		Forced Convection Heat Transfer Coefficient BTU/In.^{2}-Sec °F		Forced Convection Heat Flux BTU/In.^{2}-Sec	Average Inner Wall Temp. °F	Heat Flux At Tube Destruction BTU/In.^{2}-Sec
	Matrix	Cell X-1			Expected	Actual		Station 1	Station 5	Station 1 Inlet	Station 5 Outlet			
STANDARD HDA														
○	1	1198	30	B.O.	32	31.2	83.1	40.3	60.0	0.0148	0.0192	3.39	250	7.3
○	19	1199	30	B.O.	32	34.5	82.0	43.2	63.8	0.0128	0.0150	3.43	294	7.6
	20	1200	30	B.O.	32	32.8	78.1	41.9	64.6	0.0127	0.0120	3.55	318	14.1 (2)
○	21	1201	30	B.O.	90	89.3	75.1	98.1	119.2	0.0170	0.0123	5.049	301	5.2
○	--	1202	30	S.D.	90	92.3	75.3	99.7	115.2	0.0191	0.0211	2.39	224	- -
	2	1203	30	S.D.	90	90.3	75.3	99.1	119.9	0.0170	0.0180	3.108	281	- -
	3	1204	30	B.O.	90	91.4	76.0	97.7	112.9	0.0179	0.0147	2.333	245	5.2
+	4	1205	96	B.O.	32	35.1	84.2	43.0	64.7	0.0164	0.0210	3.362	230	6.0
+	5	1206	96	S.D.	90	89.2	78.0	99.8	119.1	0.0179	0.0175	3.026	278	- -
	6	1207	96	B.O.	90	91.3	76.0	99.4	115.9	0.0161	0.0095	2.45	307	4.5
	--	1208 (3)	62	B.O.	32	30.7	84.2	39.5	59.4	0.0151	0.0192	3.48	253	6.4
□	7	1209	55	B.O.	32	33.5	84.0	44.0	67.6	0.0149	0.0201	3.58	270	6.9
□	8	1210	55	S.D.	90	85.2	76.5	94.9	116.4	0.0192	0.0217	3.34	266	- -
	9	1211	55	B.O.	90	89.4	75.2	97.7	118.1	0.0181	0.0201	3.07	266	6.3
△	22	1212	72	S.D.	90	86.0	76.0	94.8	116.4	0.0135	0.0183	3.57	325	- -
	23	1213	72	S.D.	90	84.1	76.3	91.8	110.6	0.0146	0.0159	3.14	309	- -
	24	1214	72	B.O.	90	86.6	75.5	94.3	112.3	0.0146	0.0145	3.03	315	6.8

TABLE IV (2 of 2)

SUMMARY OF HDA HEAT TRANSFER TESTS

Symbols (4)	Test Number		Iron Impurity Level PPM Fe_2O_3	Test Type (1)	Inlet Propellant Temperature °F		Inlet Velocity FPS	Bulk Propellant Temperature		Forced Convection Heat Transfer Coefficient BTU/In.^{2}-Sec °F		Forced Convection Heat Flux BTU/In.^{2}-Sec	Average Inner Wall Temp. °F	Heat Flux At Tube Destruction BTU/In.^{2}-Sec
	Matrix	Cell X-1			Expected	Actual		Station 1	Station 5	Station 1 Inlet	Station 5 Outlet			
MODIFIED HDA (0.55% PF_5)														
○	12	1215	10	B.O.	90	95.5	73.0	101.8	122.6	0.0140	0.0225	3.08	280	7.4
○	25	1216	10	S.D.	32	33.3	81.5	42.2	64.0	0.0140	0.0183	3.026	224	- -
	10	1217	10	S.D.	32	30.5	80.0	45.2	60.5	0.0132	0.0180	3.017	253	- -
	11	1218	10	B.O.	32	37.0	80.1	45.6	66.6	0.0086	0.0180	2.935	292	8.0
○	26	1219	10	S.D.	90	94.9	69.9	103.1	133.9	0.0164	0.0193	2.961	277	- -
	27	1220	10	B.O.	90	95.2	73.3	103.0	122.4	0.0107	0.0111	2.971	382	6.9
○	15	1221	50	B.O.	90	95.5	70.9	103.2	122.4	0.0107	0.0184	2.93	280	7.1
○	13	1222	50	S.D.	32	42.6	70.2	53.5	74.7	0.0121	0.0177	3.037	264	- -
	14	1223	50	B.O.	32	44.1	78.6	55.3	77.3	0.0091	0.0125	3.115	356	7.0
◁	18	1224	97	B.O.	90	92.3	69.1	100.3	120.2	0.0107	0.0162	2.582	270	6.6
◁	16	1225	97	S.D.	32	38.7	78.2	47.8	66.2	0.0147	0.0186	3.071	248	- -
	17	1226	97	B.O.	32	39.1	79.3	47.8	67.9	0.0111	0.0185	2.932	280	8.5
	28	1227	92	B.O.	90	90.1	30.3	99.5	109.6	0.0102	0.0094	0.743	187	4.5
	29	1228	92	S.D.	90	92.9	20.4	100.1	118.7	0.0091	0.01[illegible]	1.33	240	- -
	30	1229	92	B.O.	90	87.6	30.3	91.9	104.2	0.0081	0.0080	0.808	198	5.0

NOTES:

(1) B.O. denotes burnout, S.D. denotes shutdown.
(2) CRES 347 tube used.
(3) High water content 1.5% by weight.
(4) Symbols: Reference Figure 18.